Gravitational waves from freely precessing neutron stars

D. I. Jones[★] and N. Andersson

Faculty of Mathematical Studies, University of Southampton, Highfield, Southampton SO17 1BJ

ABSTRACT

In this paper we model the gravitational wave emission of a freely precessing neutron star. The aim is to estimate likely source strengths, as a guide for gravitational wave astronomers searching for such signals. We model the star as a partly elastic, partly fluid body with quadrupolar deformations of its moment of inertia tensor. The angular amplitude of the free precession is limited by the finite breaking strain of the star's crust. The effect of internal dissipation on the star is important, with the precession angle being rapidly damped in the case of a star with an oblate deformation. We then go on to study detailed scenarios where free precession is created and/or maintained by some astrophysical mechanism. We consider the effects of accretion torques, electromagnetic torques, glitches and stellar encounters. We find that the mechanisms considered are either too weak to lead to a signal detectable by an Advanced LIGO interferometer, or occur too infrequently to give a reasonable event rate. We therefore conclude that, using our stellar model at least, free precession is not a good candidate for detection by the forthcoming laser interferometers.

Key words: accretion, accretion discs – radiation mechanisms: non-thermal – relativity – stars: magnetic fields – stars: neutron – stars: rotation.

1 INTRODUCTION

Freely precessing neutron stars have long been recognized as a potential source of detectable gravitational waves (Zimmermann 1978; Alpar & Pines 1985). Despite their regular inclusion in review articles (Thorne 1987; Flanagan 1998) they have received little in the way of detailed modelling. In this paper we will combine many of the physical processes relevant to the problem of free precession, and assess their relative importance. The motivation behind this work is to aid gravitational wave data analysis (Schutz 1991). Given the huge computational requirements of this analysis, any additional information supplied by theoretical modelling of a source greatly increases the chances of detection. With the TAMA detector already operational, the GEO600 and LIGO detectors due to go on-line within a year, and the VIRGO detector following soon after, this issue is particularly pressing.

The study of gravitational wave generation from freely precessing neutron stars can be divided into two parts. The first problem is the formulation of a free precession model consistent with our current understanding of neutron star structure. Neutron stars are not rigid bodies – they consist of a thin elastic shell containing a superfluid core. A model taking these features into account was described in detail by Jones & Andersson (2001), where the effect of free precession on electromagnetic pulsar signals was described and compared with pulsar observations.

(Several potential free precession candidates were identified, but, as we will see, they all rotate too slowly to be of gravitational wave interest.) A brief summary of this model is set out in this paper. A key feature is the decay of free precession due to dissipative processes internal to the star.

The second part of the problem is to look at particular scenarios in which free precession is created and/or maintained by an astrophysical mechanism. The torques due to accretion discs, neutron star magnetic dipole moments, and other gravitating bodies will be considered, as well as perturbations associated with glitches. We wish to investigate whether these mechanisms are capable of balancing the internal dissipation to give steady long-lived precessional motions. Having done so, we will then be in a position to estimate possible gravitational wave amplitudes in these various scenarios.

The structure of this paper is as follows. In Section 2 we briefly describe our free precession model, and parametrize the time-scale in which internal dissipation damps the wobble motion. In Section 3 we show how the finite breaking strain of the crust can be used to place an upper bound on the gravitational wave field of a precessing star, regardless of its environment. We also suggest a detection strategy for gravitational wave data analysts. General formulae relating the gravitational wave amplitude to the strength and nature of a pumping torque are given in Section 4. The possible gravitational wave field strengths in various scenarios are then estimated in Sections 5–8. Our conclusions are given in Section 9, together with some suggestions for further work.

[★]E-mail: dij@maths.soton.ac.uk

2   A MODEL OF NEUTRON STAR FREE PRECESSION

2.1   Dynamics of free precession

In this section we will briefly summarize our model of neutron star free precession. For more detail see Jones & Andersson (2001). We will begin by describing the free precession of a rigid body, as the motion in the more realistic elastic shell/fluid core case can be thought of as a modification of this.

The moment of inertia tensor of any axisymmetric rigid body can be written as

$$I = I_0 \delta + \Delta I_d (n_d n_d - \delta/3), \tag{1}$$

where δ is the Kronecker delta, and the unit vector n_d points along the symmetry axis of the body. Then the principal moments are $I_1 = I_2 = I_0 - \Delta I_d/3$ and $I_3 = I_0 + 2\Delta I_d/3$, so that $I_3 - I_1 = \Delta I_d$. When $\Delta I_d > 0$ the body is said to be *oblate*, and when negative the body is *prolate*. As we will describe below, the oblate case is the more physically plausible.
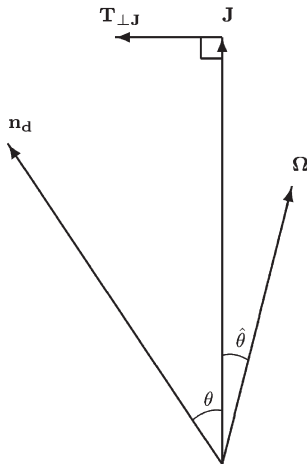
The angular momentum is related to the angular velocity according to

$$J = (I_0 - \Delta I_d/3)\Omega - \Delta I_d \Omega_3 n_d, \tag{2}$$

where the 3-axis lies along n_d. This shows that the three vectors J, Ω and n_d are always coplanar. Following Pines & Shaham (1972a,b), we will call the plane so defined the *reference plane* (see Fig. 1). Given that the angular momentum is fixed, this plane must revolve around J. The free precession is conveniently parameterized by the angle θ between n_d and J. We will refer to this as the *wobble angle*. For a nearly spherical body the angle $\hat{\theta}$ between Ω and J is much smaller than the angle between J and n_d, according to

$$\hat{\theta} \approx \frac{\Delta I_d}{I_1} \sin\theta \cos\theta. \tag{3}$$

We will denote by n_J the unit vector along J. Decomposing the

Figure 1. This figure shows the reference plane for a freely precessing body, which contains the deformation axis n_d, the angular velocity vector Ω and the fixed angular momentum J. The vectors n_d and Ω rotate around J at the *inertial precession frequency* $\dot{\phi}$. We refer to θ as the *wobble angle*. The vector $T_{\perp J}$ is the part of an applied torque that causes a secular evolution in the wobble angle.

angular velocity according to

$$\Omega = \dot{\phi} n_J + \dot{\psi} n_d \tag{4}$$

then gives

$$J = I_1 \dot{\phi}, \tag{5}$$

$$\dot{\psi} = -\frac{\Delta I_d}{I_3} \dot{\phi}. \tag{6}$$

The symmetry axis n_d performs a rotation about J in a cone of half-angle θ at the angular frequency $\dot{\phi}$. We will refer to this as the *inertial precession frequency*. There is a superimposed rotation about the symmetry axis n_d at the angular velocity $\dot{\psi}$. This is usually referred to as the *body frame precessional frequency*, with the corresponding periodicity known as the *free precession period*:

$$P_{fp} = \frac{2\pi}{\dot{\psi}}. \tag{7}$$

For a nearly spherical body, equation (6) shows that $\dot{\psi} \ll \dot{\phi}$. Note that the angles (θ, ϕ, ψ) are simply the usual Euler angles which describe the orientation of the rigid body (see, e.g., Landau & Lifshitz 1976, fig. 47).

Turning now to the more realistic case of an elastic crust with a liquid core, the moment of inertia of the crustal shell can be written as (Alpar & Pines 1985):

$$I = I_0 \delta + \Delta I_\Omega (n_\Omega n_\Omega - \delta/3) + \Delta I_d (n_d n_d - \delta/3). \tag{8}$$

The first term on the right-hand side is the moment of inertia of the non-rotating undeformed spherical shell. The second term is the change due to centrifugal forces, and has n_Ω, the unit vector along Ω, as its symmetry axis. The third term is the change due to some other source of deformation (such as strains in the crustal lattice), and has the unit vector n_d, fixed in the crust, as its symmetry axis. Without this third part the above equation would simply represent a fluid ball, and free precession would not be possible.

The free precession of such an elastic shell containing a liquid core is then very similar to the rigid result, with the geometry described in Fig. 1 still applying, provided that the ΔI_d in equations (3) and (6) is now set equal to the deformation in the inertia of the *whole* star, i.e., crust *and* core, while I_0 is still equal to the crustal moment of inertia only. Explicitly,

$$\hat{\theta} = \frac{\Delta I_d}{I_{crust}} \theta, \tag{9}$$

$$\dot{\psi} = -\frac{\Delta I_d}{I_{crust}} \dot{\phi}. \tag{10}$$

Note that centrifugal deformation ΔI_Ω is not of importance when considering the free precession geometry.

One further component can be added to our model: a pinned superfluid coexisting with the inner crust. As was first described by Shaham (1977), the effect of such a component is to increase the body-frame free precession frequency $\dot{\psi}$. In the case where the rotation rates of the superfluid and crust are the same, equations (9) and (10) still apply, with ΔI_d now containing a part equal to the moment of inertia of the pinned superfluid. However, as described in Jones & Andersson (2001), the handful of free precession candidates identified in the pulsar population do not seem to have such a component. Therefore, on those few occasions in this paper where we assume a particular source of deformation, we will assume that ΔI_d is caused entirely by Coulomb forces in the crustal lattice. (If real stars do have a significant pinned superfluid

component, then the increased body-frame precession frequency will lead to an even faster dissipation of the free precession energy, and tend to *reinforce* our final conclusion.)

The effect of a torque on the free precession can be easily summarized. Given that the torque-free motion is determined completely by the two numbers ($\dot{\phi}, \theta$), we need only describe the effect of the torque on these. If the torque causes the magnitude of the angular momentum to change at a rate $\dot{J}$, then

$$\ddot{\phi} = \frac{\dot{J}}{I_1}. \tag{11}$$

The evolution in the wobble angle is determined by the component of the torque projected into the reference plane which lies perpendicular to $\boldsymbol{J}$:

$$\dot{\theta} = -\frac{T_{\perp J}}{I_{\text{crust}} \dot{\phi}}, \tag{12}$$

as illustrated in Fig. 1.

2.2 Sources of deformation

The centrifugal deformation described above can be conveniently parameterized by the dimensionless quantity ϵ_Ω, which we will define by $3\epsilon_\Omega/2 = \Delta I_\Omega / I_{\text{star}}$ (this follows the notation of Alpar & Pines 1985). This will be of the order of the rotational kinetic energy of the star divided by its gravitational binding energy:

$$\epsilon_\Omega \approx \frac{\Omega^2 R^3}{GM} \approx 2.1 \times 10^{-3} \left(\frac{f}{100\,\text{Hz}} \right)^2 R_6^3 / M_{1.4}, \tag{13}$$

where $\Omega = 2\pi f$ is the angular frequency, R_6 the neutron star radius in units of 10^6 cm, and $M_{1.4}$ the mass in units of $1.4\,M_\odot$.

The deformation ΔI_d we can similarly parametrize in dimensionless form using the relation $3\epsilon_d/2 = \Delta I_d / I_{\text{star}}$. This deformation is due to some physical process other than rotation, which need not be specified in many of our gravitational wave estimates. However, in practice the most significant source of deformation in a neutron star is likely to be strains in its solid crust. As described in Baym & Pines (1971) and Pines & Shaham (1972a,b), if the crust has a zero strain oblateness ϵ_0, the actual deformation produced is of order

$$\epsilon_d = \frac{B}{A+B} \epsilon_0, \tag{14}$$

where the constant A depends on the stellar equation of state, and will be of the order of the gravitational binding energy of the star. The constant B also depends on the equation of state, and will be of order of the total electrostatic binding energy of the ionic crustal lattice. We will define $b = B/(A+B)$ as the *rigidity parameter*. It is equal to zero for a fluid star ($B = 0$), and unity for a perfectly rigid one ($B/A \to \infty$). Realistic neutron star equations of state imply that b takes a value

$$b \approx 1.6 \times 10^{-5} R_6^5 / M_{1.4}^3. \tag{15}$$

(See Jones 2000 for a simple derivation, and Ushomirsky, Cutler & Bildsten 2000 for a detailed numerical treatment.) The smallness of this number reflects the fact that gravitational forces dominate crustal Coulomb forces in determining the equilibrium shape of the star. In this sense, neutron star crusts are very far from perfectly rigid. Note that $b \sim 10^{-5}$ for a canonical 1.4-$M_\odot$, 10-km neutron star. More rigid stars can exist only if less massive (and therefore larger radii) neutron stars occur in nature, *or* if current equations of

state seriously underestimate the crust thickness. We will therefore present results for rigidity parameters over the interval 10^{-3} to 10^{-5}, but will bear in mind that values at the smaller end of the interval are more plausible.

For a very young star the zero-strain oblateness ϵ_0 will be determined simply by the shape of the star at the moment when its crust first solidified, i.e., $\epsilon_0 = \epsilon_\Omega(f = f_{\text{solid}})$, where f_{solid} is the spin frequency at the moment of solidification. For older stars, ϵ_0 will have changed due to plastic deformation in the crust, either because of a gradual creep, or because of a more violent shape change, possibly connected with a glitch. Certainly, it seems likely that real stars will be oblate ($\epsilon_0 > 0 \Rightarrow \Delta I_d > 0$) rather than prolate ($\epsilon_0 < 0 \Rightarrow \Delta I_d < 0$).

2.3 Wobble damping

A real neutron star, once set into free precession, will not precess forever – energy will be dissipated within the star, converting the kinetic energy of the wobble into thermal energy. Also, gravitational wave energy and angular momentum will be radiated to infinity, which must be subtracted off the star's motion.

The problem of gravitational radiation reaction was examined in detail by Cutler & Jones (2000), who showed that the main result was to cause the wobble angle to decay exponentially on a time-scale:

$$\tau_\theta = 1.8 \times 10^9 \,\text{yr} \left(\frac{I_{\text{crust}}}{10^{44}\,\text{g cm}^2} \right) \left(\frac{10^{38}\,\text{g cm}^2}{\Delta I_d} \right)^2 \left(\frac{100\,\text{Hz}}{f} \right)^4, \tag{16}$$

regardless of whether the deformation is oblate or prolate.

This is almost certainly much longer than the time-scales connected with internal dissipation. In particular, models of neutron star interiors, motivated in part by the need to model glitches, predict a frictional type coupling between the crust and core. The result of this coupling is a torque $\boldsymbol{T}$ exerted on the crust:

$$\boldsymbol{T} = K(\boldsymbol{\Omega}_{\text{fluid}} - \boldsymbol{\Omega}_{\text{solid}}), \tag{17}$$

where K is a positive constant. Such a torque would tend to restore corotation between crust and core in a glitching neutron star. However, as modelled by Bondi & Gold (1955), the torque would also tend to damp the wobble angle of a precessing body. The time-scale for this damping can be parameterized by n, the number of free precession periods P_{fp} in which one e-fold occurs:

$$\tau_d = \frac{I_0}{\Delta I_d} nP, \tag{18}$$

where P is the spin frequency (approximately $2\pi/\dot{\psi}$) of the body. The parameter n has been estimated by Alpar & Sauls (1988), who examined the scattering of electrons off the superfluid vortices. This interaction is sometimes referred to as 'mutual friction'. Alpar & Sauls estimated n to lie in the interval 400 to 10^4, giving a wobble damping time-scale of

$$\tau_d = 3.2 \,\text{yr} \left(\frac{n}{10^4} \right) \left(\frac{100\,\text{Hz}}{f} \right) \left(\frac{I_0}{10^{44}\,\text{g cm}^2} \right) \left(\frac{10^{38}\,\text{g cm}^2}{I_d} \right). \tag{19}$$

Comparing equations (16) and (19), it is clear that internal dissipation is likely to damp the free precession much more rapidly that gravitational radiation reaction.

Interestingly, in the case of *prolate* deformations, the internal dissipation acts so as to *increase* the wobble angle. However, as described in Section 2.2, prolate deformations are not likely to be found in real stars, and so for the remainder of this paper we will

assume that deformations are oblate, corresponding to a damping of the wobble motion.

3   THE GRAVITATIONAL WAVE FIELD

3.1   General form of the field

The gravitational wave field for a rigid precessing body was first calculated by Zimmerman & Szedenits (1979), using the mass quadrupole formalism (see, e.g., Misner, Thorne & Wheeler 1973). As described in the previous section, even though the elasticity and fluid core are important in determining the free precession period, the geometry of free precession in the realistic case is very similar to that in the rigid case – the deformation bulge moves in a cone of half-angle θ at a rate $\dot{\phi}$. (The superimposed rotation at $\dot{\psi}$ about the axis n_d does not change the mass quadrupole of the body, and so does not appear in the gravitational wave physics.) It follows that, to the accuracy of our model at least, the wave field calculated by Zimmerman & Szedenits (1979) applies in the realistic case. Explicitly, the gravitational waves are emitted at frequencies $\dot{\phi}$ and $2\dot{\phi}$, and with the two polarizations (denoted by $+$ and $\times$):

$$h_+(\dot{\phi}) = \frac{2\dot{\phi}^2}{r}\sin i\cos i\Delta I_{\rm d}\sin\theta\cos\theta\cos(\dot{\phi}t), \tag{20}$$

$$h_\times(\dot{\phi}) = \frac{2\dot{\phi}^2}{r}\sin i\Delta I_{\rm d}\sin\theta\cos\theta\sin(\dot{\phi}t), \tag{21}$$

$$h_+(2\dot{\phi}) = \frac{2\dot{\phi}^2}{r}(1+\cos^2 i)\Delta I_{\rm d}\sin^2\theta\cos(2\dot{\phi}t), \tag{22}$$

$$h_\times(2\dot{\phi}) = \frac{2\dot{\phi}^2}{r}2\cos i\Delta I_{\rm d}\sin^2\theta\sin(2\dot{\phi}t), \tag{23}$$

for a source at distance r and angular momentum at inclination angle i to the line of sight. Note that the $\Delta I_{\rm d}$ factor is the part of the quadrupole moment tensor due to the deformation process, *not* the centrifugal piece. The modifications to this result due to the non-rigidity are small, and lie beyond the accuracy of our free precession model.

3.2   Limit on gravitational wave amplitudes due to finite crust strength

As described in Jones & Andersson (2001), a real neutron star crust will have a finite breaking strain $u_{\rm break}$. This can be used to place an upper bound on the wobble angle of a precessing star. We know that (for small wobble angles at least) when an initially axially symmetric body is set into free precession, a deformation $\Delta I_{\rm d}$ remains along the axis n_d fixed in the star, while a deformation ΔI_Ω points along the angular velocity vector. From the point of view of an observer attached to the crust, a deformation of size ΔI_Ω describes a cone of half-angle $\theta + \hat{\theta} \approx \theta$ about n_d. This change in shape is all we need to know to estimate the strain: the change in position of any given particle is of order $R\epsilon_\Omega\theta$, while the corresponding strain is of order $\epsilon_\Omega\theta$. This precession-induced strain is not constant, but varies with magnitude $\epsilon_\Omega\theta$ over one (body frame) free precession period. As there exists a maximum strain $u_{\rm break}$ that the solid can withstand prior to fracture, the wobble angle will be limited to a value of $u_{\rm break}/\epsilon_\Omega$, so that

$$\theta_{\max} \approx 0.45\left(\frac{100\,{\rm Hz}}{f}\right)^2\left(\frac{u_{\rm break}}{10^{-3}}\right)\,{\rm rad}. \tag{24}$$

Qualitatively, we can say that more rapidly spinning neutron stars

have larger bulges to re-orientate, and therefore can sustain smaller wobble angles prior to fracture. For sufficiently slowly spinning stars the above equation breaks down, yielding angles in excess of $\pi/2$. The wobble angles of such slowly spinning stars are not limited by crustal strain.

The value of $u_{\rm break}$ is highly uncertain. By extrapolating the breaking strains of terrestrial materials, Ruderman (1992) suggests that the value relevant for neutron star crusts may lie in the range 10^{-2} to 10^{-4}.

This limit on the wobble angle θ can be used to place an upper bound on the gravitational wave amplitude of a freely precessing star with a given deformation $\Delta I_{\rm d}$. To do so, we will characterize the field strength by

$$h = \frac{G}{c^4}\frac{\dot{\phi}^2}{r}\Delta I_{\rm d}\theta. \tag{25}$$

This is an order-of-magnitude approximation to the set of equations (20)–(23). The trigonometric factor describing the variation of wave amplitude with inclination angle i has been neglected entirely, while the trigonometric factor in the precession angle θ has been replaced by its small angle limit. Note that in this small-angle limit the radiation is emitted mainly at the frequency $\dot{\phi}$ – the radiation at frequency $2\dot{\phi}$ is a factor θ smaller.

The purpose of this approximation is to enable us to gain a insight as to how gravitational wave amplitudes depend upon source parameters such as the breaking strain, frequency and deformation size. This analysis is a useful preparation for Sections 5–8, where detailed astrophysical situations are considered.

We will specialize to the case where the deformation $\Delta I_{\rm d}$ is due to Coulomb forces in the crustal lattice. We set $\Delta I_{\rm d} = 3I_{\rm star}\epsilon_{\rm d}/2$, with $\epsilon_{\rm d}$ given by equation (14). For definiteness, we will assume that the crust is 'relaxed', i.e., that the zero-strain oblateness ϵ_0 is equal to the centrifugal oblateness ϵ_Ω. (These two quantities can differ by the small crustal breaking strain anyway – see Jones & Andersson 2001.) We then find

$$h = 3.7\times10^{-28}\left(\frac{f}{100\,{\rm Hz}}\right)^4\left(\frac{b}{10^{-5}}\right)\left(\frac{{\rm kpc}}{r}\right)\theta \tag{26}$$

for a spin frequency f. In (26) θ has been left a free parameter. However, to obtain an upper bound on h, we can set θ to its maximum value as obtained from crust cracking considerations, i.e., we put $\theta = \theta_{\max}$. We then obtain

$$h(\theta = \theta_{\max}) = 3.7\times10^{-28}\left(\frac{f}{100\,{\rm Hz}}\right)^4\left(\frac{b}{10^{-5}}\right) \tag{27}$$

for $f < f_\theta$, and

$$h(\theta = \theta_{\max}) = 1.8\times10^{-28}\left(\frac{f}{100\,{\rm Hz}}\right)^2\left(\frac{b}{10^{-5}}\right)\left(\frac{u_{\rm break}}{10^{-3}}\right) \tag{28}$$

for $f > f_\theta$, where f_θ is the frequency at which $\theta_{\max} = 1$:

$$f_\theta = 69\,{\rm Hz}\left(\frac{u_{\rm break}}{10^{-3}}\right)^{1/2}. \tag{29}$$

For spin frequencies close to and below this, our small-angle approximation breaks down, so we have put $\theta = 1$ for $f < f_\theta$ so as to still obtain results correct to within an order of magnitude.

In Figs 2 and 3 we have plotted the maximum amplitude h for a variety of neutron star parameters. The noise curves have been taken from Owen & Sathyaprakash (1999). Note that a knee appears in many of the signal curves. This knee corresponds to $f = f_\theta$. Above this frequency the wobble angle is limited according
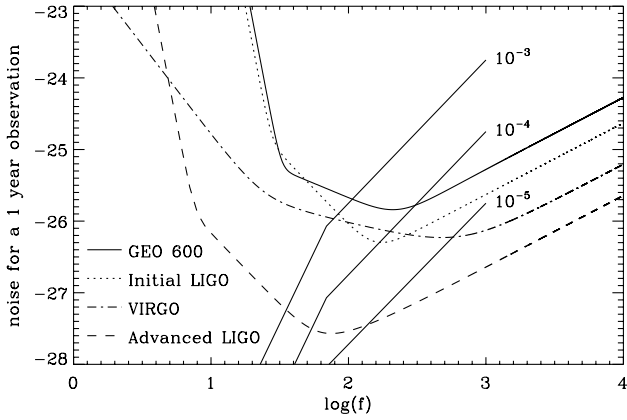
Figure 2. The maximum gravitational wave amplitude for Coulomb deformations. The star is at a distance of 1 kpc, with $u_{\text{break}} = 10^{-3}$ and $b = 10^{-3}, 10^{-4}, 10^{-5}$. The matched filter has been assumed to accumulate signal for an interval of one year. The noise curves have been taken from Owen & Sathyaprakash (1999).
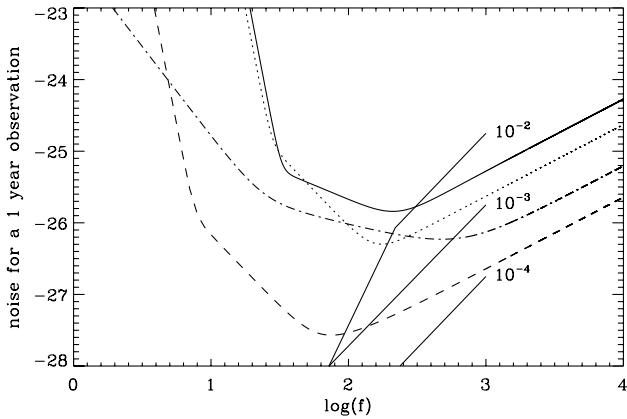
Figure 3. The maximum gravitational wave amplitude for Coulomb deformations. The star is at a distance of 1 kpc, with $b = 10^{-5}$ and $u_{\text{break}} = 10^{-2}, 10^{-3}, 10^{-4}$. The noise curves are as indicated in Fig. 2.

to (24). We have assumed that the matched filtering can accumulate signal only for a time of one year. The amplitudes are shown only for frequencies less than a kilohertz, as stars rotating more rapidly than this have not yet been observed. Fig. 2 plots h for the parameters $u_{\text{break}} = 10^{-3}$, $r = 1$ kpc and for three different values of b: $b = 10^{-5}$, $b = 10^{-4}$ and $b = 10^{-3}$. Recall that $b = 10^{-5}$ is the value expected for a canonical 1.4-$M_\odot$, $R = 10$ km neutron star, while $b = 10^{-3}$ would correspond to a lighter, larger star with a thicker crust. In Fig. 3 plots h for $b = 10^{-5}$ and breaking strains of $u_{\text{break}} = 10^{-2}, 10^{-3}$ and 10^{-4}.

In making the above assumptions regarding matched filtering, we have assumed that the wobble angle and spin frequency of the star remain constant for the observation period of one year. In practice, the wobble angle will decay significantly over this interval (see Section 2.3) unless a sufficiently strong pumping mechanism is active. However, the purpose of these figures is not to model in detail any particular scenario – they are included simply so that we might gain insight into how wave amplitudes depend upon the rigidity and breaking strain parameters, and identify parameters values capable of leading to detectable signals. These figures say nothing about the distance to the nearest source, or, in the case of burst-like sources, the event rate. Issues such as these

can be addressed only in the case of particular pumping mechanisms. This will be carried out in Sections 5–8, where the complicating effect of internal dissipation will also be included. In short, Figs 2 and 3 represent absolute upper bounds on the wave amplitude for a given spin frequency, crustal breaking strain and deformation, but give no information about likely wave amplitudes in nature.

With these qualifications in mind, we will note that these figures show that for neutron stars with $b \gtrsim 10^{-3}$, the $\theta = \theta_{\text{max}}$ gravitational wave signal is detectable by first-generation interferometers for frequencies in excess of 100 Hz. More slowly spinning sources produce steady gravitational wave signals which are intrinsically too weak to be detected. Stars with $b \approx 10^{-4}$ are potentially detectable by first-generation interferometers only for frequencies close a 1 kHz. More realistically, stars with $b \approx 10^{-5}$ are potentially detectable by an Advanced LIGO interferometer at frequencies over 100 Hz.

3.3 Detection strategy

The problem of determining source parameters from electromagnetic observations of a freely precessing neutron star was examined by Jones & Andersson (2001). The extraction of these parameters in the case of a gravitational wave detection was examined by Zimmermann & Szedenits (1979), who showed that measurement of all four components of h given in equations (20)–(23) allows extraction of the inclination angle i, the wobble angle θ and the quantity $\Delta I_{\text{d}}/r$.

As was also noted by Zimmermann & Szedenits (1979), if this is combined with an estimate of r a value for ΔI_{d} is obtained. This is of considerable use: if the deformation is of Coulomb origin, the equation $\Delta I_{\text{d}} = 3I_{\text{star}}b\epsilon_0/2$ can be combined with equation-of-state calculations of the rigidity parameter b to give the reference oblateness ϵ_0. A value of ϵ_0 very different from the fluid oblateness might then be a sign that the deformation ΔI_{d} is *not* due to crustal strains.

Note, however, that if the wobble angle is very small, the above two equations can be solved only for i and the product $\Delta I_{\text{d}}\theta/r$. This is likely to be the case for the most rapidly spinning stars, whose wobble angles are limited by fracture according to equation (24).

If the source is observed as a pulsar, it may be possible to obtain additional information. Suppose that the electromagnetic pulse originates from a dipole $\boldsymbol{m}$ inclined at an angle χ to the deformation axis. Then the motion of $\boldsymbol{m}$ is due to the combined rotation of $\boldsymbol{n_d}$ about $\boldsymbol{J}$ at $\dot\phi$ and the motion of $\boldsymbol{m}$ about $\boldsymbol{n_d}$ at $\dot\psi$. As noted by Zimmermann & Szedenits (1979), the electromagnetic pulse frequency is then given by $f_{\text{em}} = \dot\phi + \dot\psi$ for $\theta < \chi$, while for $\theta > \chi$ we have $f_{\text{em}} = \dot\phi$.

In the case of Coulomb deformations of rapidly spinning stars we would expect the $\theta < \chi$ regime to apply. Then the difference between electromagnetic and gravitational wave frequencies would give $\dot\psi$ and, to leading order, equation (10) gives

$$\Delta I_{\text{d}} = I_{\text{crust}}\dot\psi/f_{\text{em}}. \tag{30}$$

If, in addition, an estimate of the distance of the pulsar were available, the product $(\Delta I_{\text{d}}/I_{\text{crust}})\theta/r$ could be decomposed into its component parts.

The above remarks concerning frequency splitting suggest the following strategy for gravitational wave observers. Suppose we are searching for a precessional gravitational wave signal from a star of known (average) electromagnetic pulse frequency f. Then

one matched filter should be used at that frequency to cover the $\theta > \chi$ case where there is no splitting between the gravitational and electromagnetic signals. However, if splitting does occur, it will be necessary to search at a rotational frequency $\Delta f = f \Delta I_d / I_{\text{crust}}$ above this. For definiteness we will assume a Coulomb deformation to give

$$\Delta f = 3 \times 10^{-5} \left(\frac{f}{100\,\text{Hz}} \right)^3 \left(\frac{b}{10^{-5}} \right) \left(\frac{I/I_{\text{crust}}}{10} \right), \tag{31}$$

where equation (13) has been used.

We now wish to identify a frequency band in which to search for the gravitational signal. This is easily done. Consider some particular frequency, say 100 Hz. Then from Fig. 2 we see that even for an Advanced LIGO, b values less than 10^{-5} give signals too weak to be detected. From the above formula this value of b corresponds to $\Delta f = 3 \times 10^{-5}$ Hz. Therefore there is no point in searching for signals at frequencies less than $(100 + 3 \times 10^{-5})$ Hz (apart from the signal at f mentioned above). On the other hand, on physical grounds the value $b = 10^{-3}$ is surely an upper bound on the rigidity parameter. This corresponds to $\Delta f = 3 \times 10^{-3}$ Hz. Therefore there is no point in searching for signals at frequencies greater than $(100 + 3 \times 10^{-3})$ Hz. In this way we identify a frequency band in which to fruitfully search for the gravitational signal. A year-long integration would require matched filters with a 3×10^{-8} Hz spacing. In this example this would require approximately 10^5 templates.

The above argument attempts to identify the gravitational waves at the inertial precession frequency $\dot{\phi}$. There will be radiation at $2\dot{\phi}$ also. This can be searched for using templates at twice the frequencies described above.

4 CLASSIFICATION OF PUMPING MECHANISMS

It is useful to categorize pumping mechanisms according to the sort of evolution they produce in the wobble angle. As discussed above, the effect of a torque depends upon its projection into the reference plane, which rotates around the star's angular momentum vector at a rate $\dot{\phi}$. This projection will depend upon the details of the mechanism producing the torque, possibly leading to a complicated evolution in the wobble angle. Nevertheless, we will find it useful to define the four categories described below. We will define τ_{pump} as a time-scale characterizing the strength of the pumping torque. Its exact meaning will depend upon the nature of the mechanism.

It is also useful to derive the following expressions for the wave amplitude, written in terms of a time-scale rather than a frequency. Equation (25) can be combined with equation (16) to give the wave amplitude in terms of the gravitational alignment time-scale:

$$h = \left(\frac{5G}{2c^3} \frac{I_{\text{crust}}}{\tau_{g,\theta}} \right)^{1/2} \frac{\theta}{r}. \tag{32}$$

This will be extremely useful when estimating wave amplitudes for particular pumping mechanisms. Combining equation (32) with equation (24) then gives an estimate of the maximum possible wave amplitude at a given frequency and gravitational alignment time-scale $\tau_{g,\theta}$:

$$h_{\text{max}} = 1.4 \times 10^{-24} \left(\frac{I_{\text{crust}}}{10^{44}\,\text{g cm}^2} \right)^{1/2} \left(\frac{10^3\,\text{yr}}{\tau_{g,\theta}} \right)^{1/2} \left(\frac{1\,\text{kpc}}{r} \right) \tag{33}$$

for $f < f_\theta$, and

$$h_{\text{max}} = 6.7 \times 10^{-25} \left(\frac{I_{\text{crust}}}{10^{44}\,\text{g cm}^2} \right)^{1/2} \left(\frac{u_{\text{break}}}{10^{-3}} \right)$$
$$\times \left(\frac{100\,\text{Hz}}{f} \right)^2 \left(\frac{10^3\,\text{yr}}{\tau_{g,\theta}} \right)^{1/2} \left(\frac{1\,\text{kpc}}{r} \right) \tag{34}$$

for $f > f_\theta$.

In a similar way, equations (25) and (19) can be combined to give the wave amplitude in terms of the internal dissipation time-scale τ_d:

$$h = \frac{2\pi G}{c^4} I_{\text{crust}} \frac{n\dot{\phi}}{\tau_d} \frac{\theta}{r}. \tag{35}$$

Setting θ equal to its maximum value then gives

$$h_{\text{max}} = 3.3 \times 10^{-30} \left(\frac{n}{10^4} \right) \left(\frac{f}{100\,\text{Hz}} \right) \left(\frac{I_{\text{crust}}}{10^{44}\,\text{g cm}^2} \right)$$
$$\times \left(\frac{10^3\,\text{yr}}{\tau_d} \right) \left(\frac{1\,\text{kpc}}{r} \right) \tag{36}$$

for $f < f_\theta$, and

$$h_{\text{max}} = 1.6 \times 10^{-30} \left(\frac{n}{10^4} \right) \left(\frac{u_{\text{break}}}{10^{-3}} \right) \left(\frac{100\,\text{Hz}}{f} \right) \left(\frac{I_{\text{crust}}}{10^{44}\,\text{g cm}^2} \right)$$
$$\times \left(\frac{10^3\,\text{yr}}{\tau_d} \right) \left(\frac{1\,\text{kpc}}{r} \right) \tag{37}$$

for $f > f_\theta$. Again, these formulae will be of use in estimating wave amplitudes in later sections.

4.1 Oscillatory pumping

We will first consider the case where the torque does not remain fixed relative to the reference plane, but instead rotates around it at some frequency. In Sections 5 and 6 we will identify such torques that rotate at the body-frame precessional frequency with respect to the reference plane, i.e., with a frequency $\dot{\psi}$. Specializing to this case, we see that for half a precession period the wobble angle will increase, but for the next half-cycle it will decrease. We will refer to this as *oscillatory pumping*. It will produce a wobble angle that varies as

$$\theta = \theta_{\text{osc}}(1 + \cos \dot{\psi}t), \tag{38}$$

where θ_{osc} denotes the average value of θ attained. To order-of-magnitude accuracy, this will be given by

$$\theta_{\text{osc}} \sim \frac{P_{\text{fp}}}{\tau_{\text{pump}}} \sim \frac{I_{\text{crust}}}{\Delta I_d} \frac{1}{\dot{\phi}\tau_{\text{pump}}}, \tag{39}$$

where equation (10) has been used. The wave field is then estimated by substituting (39) into (25) to give

$$h \sim \frac{2\pi G}{c^4} \frac{I_{\text{crust}}}{r} \dot{\phi} \frac{1}{\tau_{\text{pump}}}. \tag{40}$$

Note that this is independent of the size of the deformation ΔI_d. However, in the case of sufficiently small ΔI_d, the precession angle as given by (39) will exceed θ_{max}. In such a case, equation (40) represents an upper bound.

4.2 Exponential pumping

In subsequent sections we will find examples of torques which tend

to increase the wobble angle at a rate proportional to the angle itself, i.e., produce *exponential pumping*. Then

$$\dot{\theta} = \theta \left(\frac{1}{\tau_{\text{pump}}} - \frac{1}{\tau_{g,\theta}} - \frac{1}{\tau_{\text{d}}} \right). \tag{41}$$

In general, these time-scales are all functions of frequency. In the case where the frequency and therefore the time-scales are not constant, the solution will be complex. However, in a constant frequency system such as an accreting star at spin equilibrium, the above equation leads to exponential solutions. We will consider such a system.

Clearly, in order to calculate the wave amplitude due to such a mechanism, we need to compare the three time-scales that appear in (41). In order to simplify this problem, we will divide it into two smaller ones. First, we will include only the pumping and gravitational radiation reaction. This will lead to an upper bound on h for stars free of internal dissipation. Then, we will include the pumping and internal dissipation only. This will lead to an upper bound on h for gravitational radiation reaction-free stars. Real stars will be acted upon by both gravitational radiation reaction and internal dissipation. Therefore, at a given frequency, the upper bound on h for real stars will be *less* than the *minimum* of the two separate bounds. In fact, we have already seen that in practice internal dissipation is more effective than gravitational radiation reaction in damping the wobble (Section 2.3). We will nevertheless include gravitational radiation reaction in this section, partly to quantify just how much weaker it is than internal damping, and partly to be able to give an upper bound on the gravitational wave amplitude that would apply even if the estimates of internal damping strength in Section 2.3 are too large by many orders of magnitude.

We begin by neglecting the internal dissipation. From equation (41) we see that θ evolves exponentially, increasing when $\tau_{g,\theta} > \tau_{\text{pump}}$ and decreasing when the inequality is reversed. The wobble angle will then either increase to its maximum value or decrease to zero:

$$\theta = \theta_{\text{max}} \quad \text{for} \quad \tau_{g,\theta} > \tau_{\text{pump}}, \quad \text{and} \tag{42}$$

$$\theta = 0 \quad \text{for} \quad \tau_{g,\theta} < \tau_{\text{pump}}. \tag{43}$$

Substitution of (42) into (32) then gives an estimate of the wave amplitude:

$$h = \left(\frac{5G}{2c^3} \frac{I_{\text{crust}}}{\tau_{g,\theta}} \right)^{1/2} \frac{\theta_{\text{max}}}{r}. \tag{44}$$

This is valid for $\tau_{\text{pump}} < \tau_{g,\theta}$, and so we obtain an *upper bound* on h if we set these two time-scales equal:

$$h(\tau_{\text{pump}} = \tau_{g,\theta}) = \left(\frac{5G}{2c^3} \frac{I_{\text{crust}}}{\tau_{\text{pump}}} \right)^{1/2} \frac{\theta_{\text{max}}}{r}. \tag{45}$$

Now consider the case where the gravitational radiation is neglected. Then equations of the form of (42) and (43) apply again, but with $\tau_{g,\theta}$ replaced by τ_{d}. Substitution into (35) then gives the estimate

$$h = \frac{2\pi G}{c^4} \frac{I_{\text{crust}}}{r} \dot{\phi} n \frac{\theta_{\text{max}}}{\tau_{\text{d}}}. \tag{46}$$

This is valid when $\tau_{\text{pump}} < \tau_{\text{d}}$, and so an upper bound is obtained when the time-scales are set equal:

$$h(\tau_{\text{pump}} = \tau_{\text{d}}) = \frac{2\pi G}{c^4} \frac{I_{\text{crust}}}{r} \dot{\phi} n \frac{\theta_{\text{max}}}{\tau_{\text{pump}}}. \tag{47}$$

4.3 Linear pumping

Now consider the case of a torque that is fixed with respect to the reference plane. Such a torque would lead to a linear variation in the wobble angle, i.e., *linear pumping*. In this case,

$$\dot{\theta} = \frac{1}{\tau_{\text{pump}}} - \theta \left(\frac{1}{\tau_{g,\theta}} - \frac{1}{\tau_{\text{d}}} \right). \tag{48}$$

We will break this up into two separate problems as above.

When the internal dissipation is neglected, we see that there is an equilibrium precession angle at which the effects of the two torques balance:

$$\theta = \frac{\tau_{g,\theta}}{\tau_{\text{pump}}}. \tag{49}$$

Substitution into equation (32) then gives the following estimate for the wave field:

$$h = \left(\frac{5G}{2c^3} I_{\text{crust}} \right)^{1/2} \frac{1}{r} \frac{\tau_{g,\theta}^{1/2}}{\tau_{\text{pump}}}. \tag{50}$$

Strictly, this is an upper bound, as when τ_{pump} is decreased below $\tau_{g,\theta}$ the precession angle as given in (49) becomes unphysically large. More precisely, the above equation represents an estimate of h for systems with $\tau_{g,\theta}/\tau_{\text{pump}} < \theta_{\text{max}}$, but an upper bound for systems where the inequality is reversed.

The analogous calculation for radiation reaction free systems gives

$$\theta = \frac{\tau_{\text{d}}}{\tau_{\text{pump}}}, \tag{51}$$

leading to the upper bound

$$h(\tau_{\text{pump}} = \tau_{\text{d}}) = \frac{2\pi G}{c^4} \frac{I_{\text{crust}}}{r} \dot{\phi} \frac{n}{\tau_{\text{pump}}}. \tag{52}$$

Clearly, the exponential and linear pumping mechanisms are very different. The exponential mechanism leads to precession only when the pumping torques overcome the radiation reaction and internal dissipation effects, i.e., either it gives wobble angles limited by θ_{max}, or it gives no precession at all. On the other hand, the linear pumping mechanism will always give a finite precession angle, as indicated in equations (49) and (51). Also, exponential pumping mechanisms cannot lead to precession in systems which are originally not precessing, whereas linear pumping mechanisms can. However, the upper bounds on h obtained via the two types of pumping are similar. Comparing (45) with (50) and (47) with (52), we see that the upper bounds differ only by a factor θ_{max}, which is of order to unity for low frequencies.

4.4 Impulsive pumping

We will describe any process that acts to increase θ on time-scales much less than a precession period as an *impulsive pumping* mechanism. For an isolated star the angular momentum during this interval will be constant (apart from any negligible amount carried away by a radiation field, unless the star ejects part of its mass!). It therefore follows that the kinetic energy of the star must change. On the other hand, if the impulse is brought about via an interaction with another body, it is possible for only the kinetic energy to change, or only the angular momentum, or both. Glitches in young pulsars are of interest as candidates for isolated impulsive pumping (Section 7), while near-body encounters in dense environments are

of interest as candidates for non-isolated impulsive pumping (Section 8).

5 ACCRETION TORQUES

Accretion torques are an obvious place to start when looking for mechanisms to pump precession. Not only are they capable of exciting wobble, but they can also maintain the spin frequency of the system, leading to the possibility of long-lived, constant wave amplitude sources. Indeed, accretion has already been investigated as a means of powering gravitational wave emission via CFS-type instabilities (Papaloizou & Pringle 1978; Wagoner 1984) and via quadrupole moment asymmetries connected with crustal composition variations (Bildsten 1998).

The torque on the central star is the sum of two parts. The first is simply the material torque, i.e., that due to the accretion of angular momentum from matter detaching from the disc and falling on to the star. The second torque is due to the coupling of the star's magnetic field with the disc. The net effect of these torques is to spin-up slowly rotating stars, but to impose a maximum spin frequency for fast stars where the accretion torque vanishes. It is useful to construct an order-of-magnitude accretion spin-up time-scale by considering the material torque at the magnetosphere radius:

$$\tau_{a,\dot\phi} \approx 1.34 \times 10^4 \, \text{yr} \left(\frac{f}{1\,\text{Hz}}\right) \left[\left(\frac{B}{10^9\,\text{G}}\right) \left(\frac{\dot M}{\dot M_\text{E}}\right)^3\right]^{-2/7} \quad (53)$$

where $\dot M$ and M_E denote the actual and Eddington accretion rates (Shapiro & Teukolsky 1983). Note, however, that this will be equal to the spin-up time-scale only for slowly rotating stars. The accretion torque will vanish when the corotation radius lies just outside the inner disc edge. This limits the spin frequency of fast stars:

$$f_\text{max} \approx 526 \, \text{Hz} \left(\frac{B}{10^9\,\text{G}}\right)^{-6/7} \left(\frac{\dot M}{\dot M_\text{E}}\right)^{3/7}. \quad (54)$$

This can be combined with equation (53) to give a lower bound on $\tau_{a,\dot\phi}$ for a given frequency and accretion rate:

$$\tau_{a,\dot\phi} \gtrsim 1.7 \times 10^3 \, \text{yr} \left(\frac{f}{1\,\text{Hz}}\right)^{4/3} \left(\frac{\dot M}{\dot M_\text{E}}\right). \quad (55)$$

If we assume that this torque has a significant component perpendicular to the star's angular momentum vector, then the corresponding wobble pumping time-scale must be I_crust/I times

this (see equation 12):

$$\tau_{a,\theta} \gtrsim 1.7 \times 10^3 \, \text{yr} \left(\frac{f}{1\,\text{Hz}}\right)^{4/3} \left(\frac{\dot M}{\dot M_\text{E}}\right) \frac{I_\text{crust}}{I}. \quad (56)$$

We will make use of this when estimating maximum wave amplitudes below.

Almost all analyses of accretion torques have assumed axisymmetry, giving rise to either purely spin-up or spin-down torques. However, precession pumping requires a torque with a component orthogonal to the spin axis. It follows that if we wish to find accretion torques capable of pumping precession, we need to identify situations in which the torque itself would be non-constant. Fortunately, we would expect this to be the case when magnetospheric effects are taken into account. As pointed out by Lamb et al. (1975), the accretion rate and therefore also the torque depend upon the balance of gravitational, centrifugal and magnetic forces. The torque is therefore a function of the plasma angular velocity, stellar angular velocity and stellar magnetic moment vectors. However, if the star is itself precessing, the relative orientation of these vectors will be modulated. This in turn must lead to a modulation of the accretion torque locked in phase with the precession. It is precisely this sort of modulation that we would expect to lead to a secular evolution in the wobble angle.

Lamb et al. (1975) demonstrated that such a modulation can be effective in exciting large-amplitude precession of a rigid body, with an excitation time-scale of the order of the spin-up time-scale, i.e., of the order of $\tau_{a,\dot\phi}$ in equation (53). For our more realistic stellar model this would correspond to an excitation on a time-scale I_crust/I times shorter. A full description of the conditions under which such pumping can occur would require a detailed understanding of the accretion process. Such a description is still not available.

To reinforce the potential complexity of this problem, the time variation of each vector involved in this problem is summarized in Table 1. Note that the vector $\boldsymbol{n}_\textbf{disc}$ describing the plane of the disc is not well defined. Far from the central star, the disc is likely to be planar. However, Vietri & Stella (1998) have argued that a non-aligned dipole will tend to lift plasma out of the disc plane. In the inner disc, viscosity will not be effective in preventing this out-of-plane motion. The inner disc will then undergo a *forced* precession, with its normal moving in a cone about the star's angular momentum.

A complete description of how this modulates the torque on the star has not been attempted previously, and lies beyond the scope of this paper. Nevertheless, it seems likely that at least part of the

Table 1. This table summarizes the temporal behaviour of the vectors of importance in the accretion problem. The final column gives their rotation rate as viewed from the inertial frame. As discussed in the text, the disc, particularly in its inner regions, may not be planar and stationary, so that $\boldsymbol{n}_\textbf{disc}$ below should be regarded as an average disc orientation. Also note that the motion of $\boldsymbol{m}$ is rather complicated – it moves on a cone of half-angle χ about $\boldsymbol{n}_d$, while $\boldsymbol{n}_d$ itself moves on a cone of half-angle θ about $\boldsymbol{J}$. These two rotations combine to give the motion of $\boldsymbol{m}$ indicated. In this case the angular velocities are average values.

Vector	Description	Motion	Frequency
$\boldsymbol{n}_\textbf{disc}$	Normal to disc	None	0
$\boldsymbol{J}$	Angular momentum of star	None	0
$\boldsymbol{\Omega}$	Angular velocity of star	Cone of half-angle $3\epsilon_d\theta/2$ about $\boldsymbol{J}$	$\dot\phi$
$\boldsymbol{n}_d$	Axis of star's deformation	Cone of half-angle θ about $\boldsymbol{J}$	$\dot\phi$
$\boldsymbol{m}$	Dipole axis	Cone, $\|\chi-\theta\| <$ half $-$ angle $< \|\chi+\theta\|$, about $\boldsymbol{J}$	$\dot\phi + \dot\psi$ for $\theta < \chi$, $\dot\phi$ for $\theta > \chi$

torque will be locked in phase with the disc precession. This torque would be most effective in exciting stellar free precession if the inner disc rotated at a rate close to the stellar spin frequency, or – more accurately – at the frequency $\dot{\phi}$. However, for all sensible parameters the Lense–Thirring precession frequency of the inner disc is much less than the star's spin frequency. This will lead to a rapid averaging of the effects of the torque on the wobble angle. It therefore seems unlikely that the forced precession of the inner disc plays a crucial role in wobble pumping. We will simply note that the notion of a single fixed disc orientation is flawed. The vector $\boldsymbol{n}_{\mathrm{disc}}$ in Table 1 should be regarded as an *average* orientation, which will describe well the outer part of the disc, but not necessarily the inner part. Given that the accretion torque may be sensitive to the relative orientation of each possible pair of vectors in Table 1, the full behaviour is complex, with the torque being modulated on a number of time-scales.

To gain a little more insight, consider the toy model where the torque on the star always points along $\boldsymbol{n}_{\mathrm{disc}}$, but has a magnitude that monotonically increases with the angle between $\boldsymbol{n}_{\mathrm{disc}}$ and $\boldsymbol{m}$. Then, by considering the relative orientation of the vectors in Table 1, it is straightforward to find a precessional phase at which the torque, when averaged over several spin periods, pumps the precession. This occurs even when the wobble angle is initially zero. However, half a precession period (i.e., $\pi/\dot{\psi}$) later the relative positions of $\boldsymbol{m}$, $\boldsymbol{n}_d$ and $\boldsymbol{J}$ have changed. Then, again when averaged over several spin periods, it is found that the wobble is either damped (if $\theta < \chi$) or pumped (when $\theta > \chi$), but this pumping is not as strong as before. This is an example of an oscillatory torque. However, the monotonicity guarantees that the pumping over one half of a precessional phase exceeds the damping over the next, giving rise to a secular increase in θ which depends on the values of θ and χ. In the limit of small wobble angles, this increase is proportional to θ, giving exponential pumping. Thus, even this simple model reproduces a number of the features identified in the general arguments above.

A more sophisticated model is provided by Wang & Robnik (1982). Here, the torque on the star is modelled using a magnetospheric interaction. The field outside of the star is the sum of the usual dipole field plus an additional field due to currents induced in the disc. This additional field is supposed to be toroidal with respect to the symmetry axis of the disc, and to be significant only near the magnetic poles of the star. Wang & Robnik then calculated the torque due to the interaction between this toroidal field and the currents internal to the star. They found that the torque on the star was qualitatively of the same form as the torque that will be considered in Section 6 when we look at electromagnetic torques on isolated pulsars. As will be shown in detail, such a torque leads to oscillatory pumping, and also to a secular evolution in θ, which for small wobble angles is exponential in nature. Again, a simple model has reproduced a number of the features identified in the general arguments.

Of course, the rather general frequency counting arguments above tell us little about the magnitude of the modulation. Neither do they say whether the precession is pumped or damped. Resolution of such issues requires a detailed model of how the torque depends on the angles involved. Nevertheless, they show that the pumping mechanism *could* apply in accreting systems. We will now consider the particular cases of exponential, linear and impulsive pumping, and investigate the gravitational wave fields they would produce.

5.1 Exponential accretion torques

In this case, equation (41) applies, with $\tau_{\mathrm{pump}} = \tau_{a,\theta}$. As described in Section 4.2, we will divide our analysis into two parts – one where internal dissipation is ignored, and the other where gravitational radiation reaction is ignored.

Begin by neglecting internal dissipation. Then arguments identical to those of Section 4.2, save for the replacement of τ_{pump} with $\tau_{a,\theta}$, lead to the upper bounds

$$h(\tau_{\mathrm{a}} = \tau_{g,\theta}) = 1.6 \times 10^{-25} \left(\frac{1\,\mathrm{kpc}}{r}\right) \left(\frac{100\,\mathrm{Hz}}{f}\right)^{2/3} \left(\frac{\dot{M}}{\dot{M}_{\mathrm{E}}}\right)^{1/2} \quad (57)$$

for $f < f_\theta$, and

$$h(\tau_{\mathrm{a}} = \tau_{g,\theta}) = 7.4 \times 10^{-26} \left(\frac{u_{\mathrm{break}}}{10^{-3}}\right) \left(\frac{1\,\mathrm{kpc}}{r}\right) \left(\frac{100\,\mathrm{Hz}}{f}\right)^{8/3}$$
$$\times \left(\frac{\dot{M}}{\dot{M}_{\mathrm{E}}}\right)^{1/2} \quad (58)$$

for $f > f_\theta$.

Now neglect gravitational radiation reaction. This leads to the upper bounds

$$h(\tau_{\mathrm{a}} = \tau_{\mathrm{d}}) = 4.3 \times 10^{-29} \left(\frac{1\,\mathrm{kpc}}{r}\right) \left(\frac{100\,\mathrm{Hz}}{f}\right)^{1/3} \left(\frac{n}{10^7}\right) \left(\frac{\dot{M}}{\dot{M}_{\mathrm{E}}}\right) \quad (59)$$

for $f < f_\theta$, and

$$h(\tau_{\mathrm{a}} = \tau_{\mathrm{d}}) = 2.0 \times 10^{-29} \left(\frac{u_{\mathrm{break}}}{10^{-3}}\right) \left(\frac{1\,\mathrm{kpc}}{r}\right) \left(\frac{100\,\mathrm{Hz}}{f}\right)^{7/3}$$
$$\times \left(\frac{n}{10^7}\right) \left(\frac{\dot{M}}{\dot{M}_{\mathrm{E}}}\right) \quad (60)$$

for $f > f_\theta$.

These curves are plotted in Fig. 4, with the values of u_{break}, r, $\dot{M}$ and n indicated by the above parameterizations. As can be seen, at all frequencies the signal is limited by the internal dissipation, despite the high value of n assumed (three orders of magnitude larger than the largest value estimated by Alpar & Sauls 1988). We therefore see that the wave amplitude due to exponential pumping
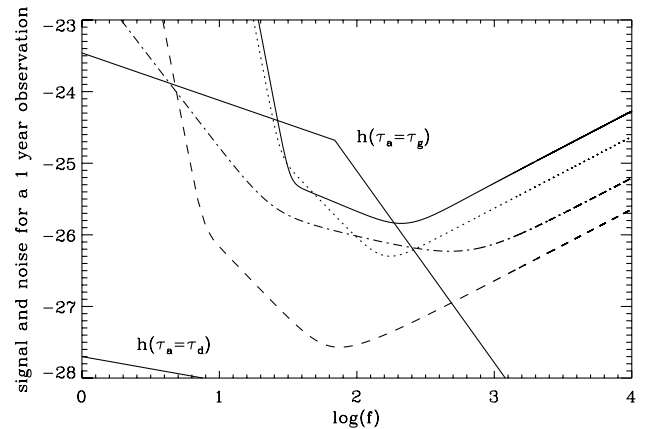
Figure 4. The maximum wave amplitude for an accreting star when secular accretion torques act. We have assumed $u_{\mathrm{break}} = 10^{-3}$, $r = 1\,\mathrm{kpc}$, and accretion at the Eddington rate. The curve $h(\tau_{\mathrm{a}} = \tau_{g,\theta})$ is the bound from balancing gravitational and accretion torques. The curve $h(\tau_{\mathrm{a}} = \tau_{\mathrm{d}})$ is the bound from balancing internal dissipation and accretion torques, with $n = 10^7$.

by accretion torques is almost certainly limited to undetectable values by internal dissipation. We will not consider this mechanism any further.

5.2 Linear accretion torques

In this case, equation (48) applies, with $\tau_{\text{pump}} = \tau_{a,\theta}$. This will lead to upper bounds on h that coincide with the low-frequency portions of the curves in Fig. 4. Therefore internal dissipation still limits the amplitude to undetectable values.

5.3 Impulsive accretion torques

We will now discuss a pumping mechanism that will apply even in the absence of the gating described previously. Suppose that the accreting plasma is clumped, and is not entirely confined to the plane perpendicular to the star's rotation axis. Various instabilities are likely to lead to such a situation, as discussed in Lamb et al. (1985). Indeed, the clumping of accreting plasma is a key ingredient of the 'beat-frequency' models. These ascribe the quasi-periodic oscillations observed in many X-ray systems to a variability in the accretion rate. This variability is due to a beating between the frequency of the innermost stable orbit and the star's spin frequency. It therefore seems likely that the phenomenon of clumping in accreting systems is generic.

Denote by Δt_1 the (average) time-scale in which a clump transfers its angular momentum to the star. The wobble angle will change impulsively due to the accretion of such clumps, provided that the transfer of angular momentum takes place over a narrow range of rotational phase, i.e., provided that $\Delta t_1 \ll P$, where P denotes the star's spin period. If, in addition, the clumps arrive at random time intervals of average Δt_2, then, provided that $P_{\text{fp}} \ll \Delta t_2$, a random walk in θ will occur, even though no gating occurs. In the absence of gravitational radiation reaction and internal damping the wobble angle will then grow as $t^{1/2}$. This is clearly a less effective pumping mechanism than the linear one considered previously, and so it will not lead to an interesting gravitational wave amplitude.

6 ELECTROMAGNETIC TORQUES

Models of the electromagnetic torque on a spinning neutron star have split into two classes. The first is the Goldreich & Julian (1969) model where a dipolar magnetic field embedded in the star generates a strong electric field at the stellar surface which rips out charged particles. These then propagate along the magnetic field lines, forming a magnetosphere. This applies even when the dipole and rotation axes coincide. The radiation the charged particles emit then carries energy away from the star, implying the existence of a braking torque.

The second class does not have a magnetosphere, and instead models the star as a perfect conductor with a magnetic dipole embedded, surrounded by vacuum (Ostriker & Gunn 1969). If the dipole is inclined to the rotation axis, electromagnetic radiation at the spin frequency is emitted. This provides the braking torque. Such models are clearly oversimplified. However, the magnetosphere models are so complicated that very little progress has been made in understanding their details (Michel 1991); questions such as how the electromagnetic torque depends upon the angle between the spin axis and dipole axis remain unanswered. Therefore, in this section we will look at a magnetosphere-free model in which the torque has been calculated as a function of the spin and dipole

moment vectors. Even though the details of such a model may prove to be incorrect, it is likely that it will reproduce qualitatively many features of real stars, and in particular identify the important time-scales involved.

Most discussions of magnetosphere-free torques are based on the model of Deutsch (1955), who considered a perfectly conducting sharply bounded sphere, rigidly rotating in a vacuum. The internal magnetic field was assumed to be symmetric about some axis inclined to the axis of rotation. The external magnetic and electric fields were then calculated. These fields were then used by Davis & Goldstein (1970) and Michel & Goldwire (1970) to calculate the torque on the star. These authors investigated the effect of this torque on spherical stars. They were able to show that the torque caused the magnetic dipole to align with the rotation axis on the electromagnetic spin-down time-scale.

Goldreich (1970) extended the analysis to examine the effect of torques on precessing bodies. He showed that when the free precession period was less than the electromagnetic spin-down time-scale, the non-sphericity completely altered the body's evolution – the magnetic moment no longer aligns with the spin axis. Instead, the torque serves to either pump or damp any free precession the body may be undergoing, depending upon whether the angle χ between the dipole moment and the body's deformation axis is greater or smaller than $\sin^{-1}(2/3)^{1/2} \approx 55°$, respectively. We will refer to this process as the *Goldreich mechanism*. This is very different from the gravitational radiation reaction case, in which the wobble motion is always damped (Cutler & Jones 2000).

The issue of calculating the electromagnetic torque was taken up again by Good & Ng (1985). Much of their analysis was concerned with Goldreich–Julian type magnetosphere torques. However, in the course of their calculation they found an error in the Deutsch fields. When this is taken into account, the Deutsch vacuum torque T is given by:

$$T \equiv T_1 + T_2 = \frac{2\Omega^2}{3c^3}(\boldsymbol{\Omega} \times \boldsymbol{m}) \times \boldsymbol{m} - \frac{1}{5Rc^2}(\boldsymbol{\Omega} \cdot \boldsymbol{m})(\boldsymbol{\Omega} \times \boldsymbol{m}), \quad (61)$$

where $\boldsymbol{\Omega}$ denotes the angular velocity, R the stellar radius, and $\boldsymbol{m}$ the dipole moment. (The only difference between this and the torque as calculated from the original Deutsch paper is a factor of $-1/5$ in T_2.)

The first term, T_1, has components both parallel and perpendicular to the spin axis, and scales as Ω^3. It is known as a *non-anomalous* torque. It causes the energy and angular momentum of the star to decrease. Its component parallel to J is responsible for spin-down, while its component perpendicular to J will bring about a secular change in the wobble angle.

The second term, T_2, is exactly perpendicular to the angular velocity, and scales as Ω^2. It is known as an *anomalous* torque, and is caused by the near-zone fields. It does not lead to a loss in energy or angular momentum. This torque does affect the wobble angle and spin rate of a freely precessing star, but its effects average to zero over one free precession period.

Following equation (61), we will define two time-scales to characterize the torque. The first corresponds to T_1 and is simply the spin-down time-scale $f/\dot{f} = 3Ic^3/2R^6\dot{\phi}^2B^2$:

$$\tau_e = 3.64 \times 10^3 \text{ yr} \left(\frac{10^{12}\,\text{G}}{B}\right)^2 \left(\frac{100\,\text{Hz}}{f}\right)^2 \left[\frac{1}{\sin^2\chi}\right]. \quad (62)$$

The corresponding time-scale on which this torque would evolve the wobble angle is I_{crust}/I shorter than this. In the above formula, and those that follow, we will place the geometric factors that

follow from the particular form of vector and scalar products of equation (61) in square brackets. In this way it will be clear what conclusions can be drawn if only the approximate time-scales of the model hold, i.e., if in more realistic magnetosphere models the above geometric factors were found to be incorrect. Such a situation would correspond to replacing the term in square brackets with some other geometric factor.

The second time-scale corresponds to T_2 and we define as

$$\hat{\tau}_{\mathrm{e}} = 76.2 \, \mathrm{yr} \left(\frac{10^{12} \, \mathrm{G}}{B} \right)^2 \left(\frac{100 \, \mathrm{Hz}}{f} \right) \left[\frac{1}{\sin^2\chi} \right]. \tag{63}$$

It is a factor $\Omega R/c$ shorter than τ_{e}. Again, the corresponding time-scale on which this torque would evolve the wobble angle is I_{crust}/I shorter than this.

Thus the effects of the two torque terms are qualitatively different. The term T_1 results in a secular variation in the free precession angle and spin rate on the electromagnetic spin-down time-scale. The term T_2 produces no such secular variation. Instead, it causes oscillations in the spin frequency and wobble angle on the (much shorter) free precession time-scale. We will refer to this as a *non-secular* mechanism. We will examine both torques in terms of their effect on gravitational wave generation below.

6.1 Non-secular electromagnetic torques

The torque T_2 has received very little attention previously, undoubtedly because it does not cause any secular variation in the star's motion. However, as can be deduced from equation (61), its magnitude and orientation with respect to the reference plane vary over one precession period, as m rotates with respect to this plane. Recently, Melatos (1999) made use of this torque to model spin-down irregularities in magnetars, modelled as rigid bodies. He considered the case where the time-scale $\hat{\tau}_{\mathrm{e}}$ was of similar duration to the free precession period: $\hat{\tau}_{\mathrm{e}} \sim P_{\mathrm{fp}}$. This similarity of time-scales gives a rather irregular or 'bumpy' spin-down rate, which Melatos calculated numerically. We will take a somewhat simpler view – when $\hat{\tau}_{\mathrm{e}}$ is longer than P_{fp}, the effect of the torque will be simply to cause a smooth variation of free precession parameters (e.g., θ and $\dot{\phi}$), calculable using perturbation theory. Even when the two time-scales become comparable we would expect our results to apply to order-of-magnitude accuracy.

Substitution of T_2 into (12) shows that for small wobble angles, θ varies sinusoidally, giving oscillatory pumping of the form discussed previously. An estimate of the magnitude of this angle follows from the time-scale $\hat{\tau}_{\mathrm{e}}$ described above:

$$\theta_{\mathrm{ns}} \sim \frac{P_{\mathrm{fp}}}{\hat{\tau}_{\mathrm{e}} I_{\mathrm{crust}}/I}. \tag{64}$$

From equation (40) this leads to a wave field

$$h \sim \frac{G\pi}{2c^4} \frac{I_0}{r} \dot{\phi}^2 \frac{1}{\hat{\tau}_{\mathrm{e}}}. \tag{65}$$

This gives

$$h = 1.8 \times 10^{-28} \left(\frac{1 \, \mathrm{kpc}}{r} \right) \left(\frac{1 \, \mathrm{yr}}{\tau_{\mathrm{e}}} \right) \left[\frac{3}{5\pi} \frac{1}{\tan^2\chi} \right], \tag{66}$$

where we have parameterized in terms of τ_{e} rather than $\hat{\tau}_{\mathrm{e}}$. As above, the geometric factor deduced from the full perturbative calculation has been separated from the rest of the formula.

Clearly, this is extremely weak. The amplitude increases as the

electromagnetic spin-down time-scale decreases, so we should focus attention on fast spinning strongly magnetized stars, i.e., stars very soon after birth in supernovae. Such stars will be hot, with temperatures of order $10^{11} \, \mathrm{K}$ immediately after birth. However, this mechanism can become active only when the outer phase has solidified to form a crust, and so we can apply equation (66) only to stars which cool to the melting temperature in a time less than τ_{e}.

As described in Haensel (1997), the crust will not have a single well-defined melting temperature, as the deeper parts (with density $\sim 10^{13} \, \mathrm{g \, cm^2}$) will melt at temperatures just under $10^{10} \, \mathrm{K}$, while the outer crust (with density $\sim 10^{11} \, \mathrm{g \, cm^2}$) will melt at temperatures just above $10^9 \, \mathrm{K}$. There is therefore some ambiguity in what to take as an average melting temperature, with a corresponding ambiguity in the time-scale for crust formation. For the range of temperature identified, an upper bound would be one year, with a lower bound much shorter than this (Haensel 1997; Shapiro & Teukolsky 1983).

If the solidification time-scale is indeed of order one year, equation (66) then leads to the tiny signal of order 10^{-29} for a star born at the Galactic Centre. To be detectable over a one-year integration, the geometric factor would have to exceed 10^2, corresponding to very small dipole inclination angles, $\chi < 2°$.

If the star's outer layers were to cool more rapidly than this, we can consider the effective amplitude found by multiplying the wave amplitude by the square root of the number of revolutions performed in one electromagnetic braking time-scale:

$$h_{\mathrm{eff}} = 2.5 \times 10^{-26} \left(\frac{1 \, \mathrm{kpc}}{r} \right)$$
$$\times \left(\frac{1 \, \mathrm{yr}}{\tau_{\mathrm{e}}} \right)^{1/2} \left(\frac{f}{100 \, \mathrm{Hz}} \right)^{1/2} \left[\frac{3}{5\pi} \frac{1}{\tan^2\chi} \right]. \tag{67}$$

Even with fast (less than one-year) cooling, a star born at the Galactic centre remains undetectable unless the geometric factor amplifies the signal. A dipole inclination of $5°$ gives an amplification of 25. At $100 \, \mathrm{Hz}$ the signal is detectable for $\tau_{\mathrm{e}} = 1$ month, and a polar magnetic field of $2 \times 10^{15} \, \mathrm{G}$. Such an event could correspond to the birth of a magnetar. However, the event rate for such an occurrence is very low – surely less than one a century, so that the probability of such a source being born during the operational lifetime of Advanced LIGO is small.

The torque T_2 is due to the near-zone fields and does not lead to energy being radiated to infinity. Therefore it is conceivable that it may continue to act in an accreting system. In this case the spin frequency would be maintained by the accretion torque. To obtain an upper bound on the wave field at a given frequency, set τ_{e} equal to its minimum value as given by combining (54) and (62):

$$\tau_{\mathrm{e}} = 3.4 \times 10^7 \, \mathrm{yr} \left(\frac{f}{100 \, \mathrm{Hz}} \right)^{1/3} \left(\frac{\dot{M}}{\dot{M}_{\mathrm{E}}} \right)^{-1}. \tag{68}$$

Substituting this into equation (66) gives a maximum wave amplitude of

$$h_{\mathrm{max}}(f) = 2.4 \times 10^{-36} \left(\frac{1 \, \mathrm{kpc}}{r} \right) \left(\frac{100 \, \mathrm{Hz}}{f} \right)^{1/3} \left(\frac{\dot{M}}{\dot{M}_{\mathrm{E}}} \right). \tag{69}$$

This is tiny even in comparison to the wave amplitudes from isolated stars. This is because in accreting systems the two factors which give large wave amplitudes – high spin frequency and high polar magnetic field strength – compete. Highly magnetized stars have large Alfvén radii and therefore low equilibrium spin rates.

To sum up, the non-secular electromagnetic torque does not

seem to be a good pumping mechanism for gravitational wave generation. Isolated stars at the Galactic centre with high spin frequencies and large magnetic field strengths can produce detectable signals if the geometric factors which enter the calculation are favourable. However, if born in supernovae, their rapid spin-down rates would require extremely fast (less than one-year) cooling of the outer phases of the star. Accreting stars where this near-zone torque continues to act produce even smaller gravitational wave signals, as the requirements of high spin frequency and high magnetic field strength oppose.

6.2 Secular electromagnetic torques

Having investigated the non-secular effect of electromagnetic torques on gravitational wave generation, we will now consider the possibility that such torques may pump precession in a secular way. Goldreich (1970) demonstrated that the torque T_1 of equation (61) does indeed lead to such evolution for a rigid body. This generalizes at once to our elastic shell/fluid core model. Substitution of T_1 into equations (11) and (12) leads to a set of two coupled differential equations connecting $\dot{\phi}$ and θ. Provided that the free precession period is less than the spin-down time-scale, we can average over a free precession period to give:

$$\ddot{\phi} = -\alpha\dot{\phi}^3 \sin^2\chi, \tag{70}$$

$$\dot{\theta} = \frac{I}{I_{\text{crust}}}\alpha\dot{\phi}^2\theta\left[\frac{3}{2}\sin^2\chi - 1\right], \tag{71}$$

where

$$\alpha = \frac{2m^2}{3Ic^3}. \tag{72}$$

(Small terms proportional to $\Delta I_d/I_{\text{crust}}$ and θ^2 have been neglected.) Then the spin-down follows the usual power law:

$$\dot{\phi} = \dot{\phi}_0\left(1 + \frac{2\sin^2\chi t}{\tau_e}\right)^{-1/2}, \tag{73}$$

where τ_e is defined in equation (62). The wobble angle evolves according to

$$\theta = \theta_0\left(1 + \frac{2\sin^2\chi t}{\tau_e}\right)^\lambda, \tag{74}$$

where

$$\lambda = \frac{I}{I_{\text{crust}}}\frac{\frac{3}{2}\sin^2\chi - 1}{2\sin^2\chi}. \tag{75}$$

As can be seen, θ increases or decreases depending upon the sign of $\frac{3}{2}\sin^2\chi - 1$, and increases most rapidly for $\chi = 90°$, in which case

$$\theta(\chi = 90°) = \theta_0\left(1 + \frac{2t}{\tau_e}\right)^{I/4I_{\text{crust}}}. \tag{76}$$

In reality, gravitational radiation reaction and internal dissipation will act on the spinning down star also, and so we should include their effects. Then equations (70) and (71) acquire extra terms. The gravitational spin-down of equation is added to (70), while the gravitational alignment of equation (16) is added to (71). The internal dissipation alignment rate corresponding to equation (19) is added to (71).

We will present the $\chi = 90°$ results where the electromagnetic pumping is greatest:

$$\ddot{\phi} = -\alpha\dot{\phi}^3 - \beta\dot{\phi}^5\theta^2, \tag{77}$$

$$\dot{\theta} = \frac{1}{2}\frac{I}{I_{\text{crust}}}\alpha\dot{\phi}^2\theta - \beta\frac{I}{I_{\text{crust}}}\dot{\phi}^4\theta - \frac{\Delta I_d}{I_{\text{crust}}}\frac{\dot{\phi}}{2\pi n}\theta, \tag{78}$$

where

$$\beta = \frac{2G}{5c^5I}\Delta I_d^2. \tag{79}$$

The terms proportional to α are due to electromagnetic torques, those proportional to β to gravitational torques, and the term proportional to n^{-1} describes internal damping. In terms of time-scales, equation (78) would be written

$$\dot{\theta} = \theta\left(\frac{1}{\tau_{e,\theta}} - \frac{1}{\tau_{g,\theta}} - \frac{1}{\tau_d}\right), \tag{80}$$

where for convenience we have introduced the electromagnetic wobble pumping time-scale

$$\tau_{e,\theta} = 2\tau_e\frac{I_{\text{crust}}}{I}. \tag{81}$$

Note that the time-scales in this problem are functions of the decreasing frequency, so this equation will generally not have simple exponential solutions.

We will apply this formalism to a young rapidly spinning-down neutron star. Its initial wobble may be due to glitches arising from the rapid spin-down (Section 7), or due to some other process. We will not concern ourselves with this issue here. We will simply examine the evolution of the precession angle, assuming that the Goldreich mechanism acts.

Fortunately, it is possible to simplify the above equations somewhat. First, the gravitational radiation reaction time-scale for spin-down is much longer than for gravitational alignment, so in any situation where the time-scales in (80) are similar the gravitational spin-down term is negligible, i.e., the last term of (77) may be neglected. Also, the damping due to gravitational radiation reaction will be much weaker than the damping due to internal dissipation. Then the second term of (78) may be neglected.

For such a star the evolution in $\dot{\phi}$ is driven only by the electromagnetic torque and equation (73) applies. The evolution in θ is more complex. Integration of (78) depends on the variation of ΔI_d with the frequency. We will consider the case of Coulomb deformations, and assume $\Delta I_d \propto \dot{\phi}^2$ (i.e., that the crust is relaxed). We then find

$$\theta = \theta_0\left(1 + \frac{2t}{\tau_e}\right)^{I/4I_{\text{crust}}}\exp\left\{\frac{\tau_e}{6\tau_d}\left[\left(1 + \frac{2t}{\tau_e}\right)^{-1/2} - 1\right]\right\}. \tag{82}$$

We can now build up a picture of the evolution of a star which is acted upon by a secular electromagnetic torque of this form. The scaling of the time-scales with frequency are crucial: $\tau_d \propto 1/\Delta I_d\dot{\phi} \propto 1/\dot{\phi}^3$, while $\tau_e \propto 1/\dot{\phi}^2$. If the star is born spinning sufficiently fast, the steeper dependence of τ_d on frequency will give $\tau_d \ll \tau_e$, and the above equation reduces to

$$\theta \approx \theta_0\exp\left(-\frac{t}{\tau_d}\right). \tag{83}$$

As the star continues to spin down, the two time-scales become comparable, and eventually θ will begin to increase. At late times equation (6.2) reduces to

$$\theta \approx \left[\theta_0\exp\left(-\frac{\tau_e}{\tau_d}\right)\right]\left(1 + \frac{2t}{\tau_e}\right)^{I/4I_{\text{crust}}}. \tag{84}$$

This is of the same form as (76), save for the extra exponential factor. This factor can be interpreted as the extent to which the wobble was damped early in the life of the star. An example of this
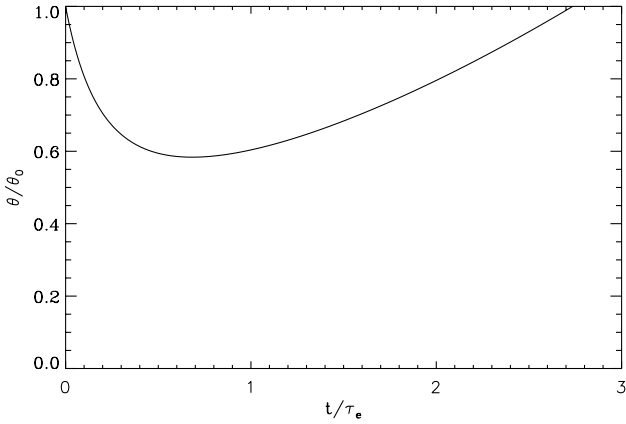
Figure 5. The evolution in the wobble angle θ under the action of combined internal dissipation and electromagnetic torques. We have put $\tau_e = 0.13 \times \tau_{g,\theta}$. At early times the internal dissipation dominates and θ decreases exponentially. At later times the electromagnetic torque dominates and θ increases as $(1 + 2t/\tau_e)^{I/4I_{crust}}$.

behaviour is shown in Fig. 5. Time is measured in units of τ_e, and we have chosen $\tau_d = 0.13\tau_e$. An example of such a star where Coulomb forces provide the distortion could have $b = 10^{-5}$, $I_{crust}/I = 0.1$, $B = 10^{13}$ G and an initial spin frequency of 200 Hz. Then $\tau_e = 9$ yr. The initial exponential decrease in θ, on a time-scale of approximately one year, is clearly seen. Of course, this neglects the possibility that a CFS-type instability (such as an r-mode) might rapidly brake the star's rotation (Andersson & Kokkotas 2001).

In this way, electromagnetic radiation reaction could provide a way of setting young neutron stars into free precession. Given some initial non-zero wobble angle and the condition $\tau_{e,\theta} < \tau_d$, the wobble angle increases. Of course, this increase will end when θ reaches the maximum value as set by the crustal breaking stress. From that point on, the wobble angle will remain fixed at its maximum value, while the spin frequency continues to decrease according to equation (73). The gravitational wave amplitude is proportional to $\Delta I_d \dot{\phi}^2$. Given our assumption $\Delta I_d \propto \dot{\phi}^2$, this leads to a wave amplitude proportional to $\dot{\phi}^4$, which in turn evolves as $(1 + 2t/\tau_e)^{-2}$. In other words, for all but the earliest stages of evolution the gravitational wave amplitude decreases steadily with time – we have been able to maintain a non-zero wobble angle only at the expense of introducing a powerful spin-down torque. The gravitational wave amplitude decreases on a time-scale of order τ_e. In Section 7 we will look at the wave field due to a population of young *unmagnetized* isolated stars, set into free precession at (or very soon after) birth, whose precession angles then decay on the internal damping time-scale τ_d. Given that the wave field of the magnetized stars considered in this section decays on the time-scale $\tau_{e,\theta} < \tau_d$, the magnetized stars are not as easily detectable, and so we will not pursue them further. Rather, in Section 7 we will consider in detail the signal strength and population statistics of young unmagnetized stars, and find that for realistic values of the damping parameter n, detection of such a population is not likely.

To summarize, this non-secular electromagnetic pumping can increase the wobble angle of an isolated star. However, once the wobble angle has increased to its maximum value, the associated spin-down torques dominate the evolution in the wave signal, with the result that the amplitude decreases on the electromagnetic spin-down time-scale.

This motivates us to consider the possibility that secular electromagnetic pumping remains active even in an accreting system: the accretion torque could then maintain the star's spin frequency, while the electromagnetic torque maintains the free precession. It is more difficult to justify this combining of accretion and electromagnetic torques than in the case of the non-secular electromagnetic torque, as a secular variation in θ changes the energy and angular momentum of the star, and so must correspond to fluxes of energy and angular momentum to infinity. Certainly it is clear that the exact form of the torque $\mathbf{T_1}$ will no longer apply, as its spin-down part at least will be suppressed by the accretion environment. We will therefore dispense with the details of the above, i.e., the χ and numerical factors, and will assume that the star is in spin equilibrium, as described by standard accretion theory. Then the star is modelled by

$$\dot{\theta} = \theta \left(\frac{1}{\tau_e} - \frac{1}{\tau_{g,\theta}} - \frac{1}{\tau_d} \right), \tag{85}$$

$$\ddot{\phi} = 0. \tag{86}$$

The time-scales in (85) are constant by virtue of (86), and so the solution will be exponential in form. However, we now have to include the details of the accretion spin-up torque, the electromagnetic pumping torque, and internal dissipation. In fact, it is possible to combine formulae describing these three phenomena to obtain an upper bound on the gravitational wave signal, independent of the mechanism producing the deformation. First, we can combine equation (62) for the electromagnetic spin-down time with equation (54), which gives the maximum spin frequency of a star with a given magnetic fields strength and a given accretion rate. This provides the lower bound on τ_e given by equation (68). However, for the Goldreich mechanism to be operative, we must have $\tau_{e,\theta} = 2\tau_e I_{crust}/I < \tau_d$. The above equation can then be used to give a lower bound on τ_d, at a given spin frequency, accretion rate and value of I_{crust}/I. However, $\tau_d \propto I_{crust}/\Delta I_d$, and so we obtain an upper bound on ΔI_d. This immediately become an upper bound on the gravitational wave amplitude. Carrying out the arithmetic, we find:

$$h(\tau_e = \tau_d) = 5.0 \times 10^{-31} \left(\frac{\dot{M}}{\dot{M}_E} \right) \left(\frac{f}{100\,\text{Hz}} \right)^{2/3} \left(\frac{n}{10^7} \right) \left(\frac{1\,\text{kpc}}{r} \right) \tag{87}$$

for $f < f_\theta$, and

$$h(\tau_e = \tau_d) = 2.4 \times 10^{-31} \left(\frac{u_{break}}{10^{-3}} \right) \left(\frac{\dot{M}}{\dot{M}_E} \right) \left(\frac{100\,\text{Hz}}{f} \right)^{4/3}$$
$$\times \left(\frac{n}{10^7} \right) \left(\frac{1\,\text{kpc}}{r} \right) \tag{88}$$

for $f > f_\theta$. This is a tiny amplitude. Even for $n = 10^7$, it reaches a maximum of only 10^{-30}, at a frequency of 69 Hz for the values of u_{break} chosen. Therefore the gravitational wave amplitude of accreting stars acted upon by electromagnetic torques of this form is limited to uninteresting values by internal dissipation.

To conclude, secular electromagnetic torques are not likely to lead to detectable levels of gravitational radiation. In the case of isolated stars the torque may be able to increase an initially small wobble angle to its maximum value, but only at the expense of introducing a strong spin-down torque. Even if this part of the torque were to remain active in accreting stars, the wave amplitudes are uninteresting. The bound on h obtained by considering the competition between the electromagnetic torque

and the internal dissipation time-scale leads to a bound on h much lower than even the Advanced LIGO sensitivity. We will therefore not consider the effects of electromagnetic torques any further.

7 NATAL PRECESSION AND GLITCHES

Given their violent birth in supernovae, it is tempting to examine the possibility that neutron stars are set into precession when born. As discussed in Section 6.1, the high temperatures generated by the implosion will lead to entirely fluid stars. Only when the outer layers have cooled will a solid crust form. It is possible that when the crust is in the process of solidifying a substantial excitation of a mode of oscillation of the fluid exists. This excitation could simply be due to the supernova explosion itself, or could be due to a CFS-type instability. Such a scenario has already been investigated in the context of r-modes, where the crust formation was a hindrance to gravitational wave emission (Andersson et al. 2000; Lindblom, Owen & Ushomirsky 2000). The exact outcome is not clear, particularly as the crust will not solidify at all points simultaneously, but will form first where the fluid velocity is smallest. Given the complexity of the process, the possibility of the crust/fluid core system being created in a precessional state cannot be ruled out.

Even if the star has settled down into an axisymmetric configuration at the time of crust solidification, it is possible that it might be set into free precession soon after. As noted by Lyne (1996), the phenomenon of glitching – the sudden increase in spin frequency of a pulsar – is most common in young pulsars. This phenomenon certainly requires a solid crust. Therefore a young neutron star that has cooled sufficiently will begin to glitch. Also, some theories of glitching associate the sudden change in spin frequency with a fracture in the crustal structure (see Ruderman 1976, 1991a,b and Link, Franco & Epstein 1998 for details). If this change results in a shift in the principal axis of the moment of inertia tensor, the star will precess (Pines & Shaham 1973a,b; Link et al. 1998). In this way it is possible that stars may acquire a precessional motion very soon after birth.

We therefore wish to investigate the gravitational wave background due to a population of young spinning-down neutron stars that were set into precession at, or soon after, birth. We will describe this as *natal precession*. Although we have identified fluid modes and glitches as possible ways of producing this natal precession, the following analysis would apply regardless of the source of the wobble.

7.1 Gravitational wave amplitudes

We will not include any pumping mechanisms in our analysis, so that the wobble angle simply decays under the combined influence of internal dissipation and gravitational radiation reaction. Also, we will begin by considering stars for which electromagnetic spin-down torques are negligible. We would then have

$$\dot{\theta} = -\theta\left(\frac{1}{\tau_{g,\theta}} - \frac{1}{\tau_d}\right) \equiv -\frac{\theta}{\tau}. \tag{89}$$

If we set the initial wobble angle equal to its maximum value, we have

$$\theta(t) = \theta_{max} \exp\left(-\frac{t}{\tau}\right) \tag{90}$$

for $t > 0$, and zero for $t < 0$.

In order to gain insight into the detectability of the gravitational wave field due to such a source, we shall assume that a matched filter can accumulate signal only for an interval τ or for an interval of one year, whichever is shorter. Figs 6 and 7 show the effective amplitude for a star deformed by crustal Coulomb forces, with a strain angle $u_{break} = 10^{-3}$, at a distance of 1 kpc. Each figure plots h for three different values of the rigidity parameter: $b = 10^{-3}$, 10^{-4} and 10^{-5}. We have assumed a reference oblateness equal to that of a rotating fluid, i.e., $\epsilon_0 = \epsilon_\Omega$, so that $\Delta I_d = 3I_{star}b\epsilon_\Omega/2$. In Fig. 6, only the gravitational radiation reaction term of equation (89) is included, i.e., this is the $n \to \infty$ limit. Fig. 7 has $n = 10^4$, which is the upper bound on n based on the arguments of Alpar & Sauls (1988). This level of damping reduces the signal significantly as compared to Fig. 6 for frequencies in excess of 100 Hz. For example, a $b = 10^{-3}$ star is now barely detectably by a first-generation interferometer, while the more plausible $b = 10^{-5}$ star is now barely detectable by an Advanced LIGO.
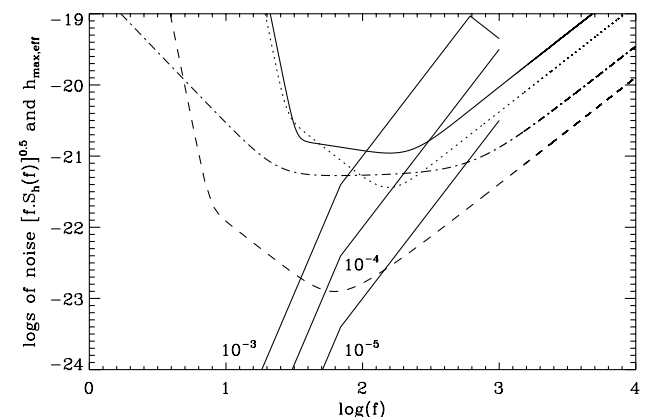
Figure 6. The effective amplitude from an isolated star which initially precesses at its maximum wobble angle with damping due to gravitational radiation reaction only. We have put $u_{break} = 10^{-3}$ and $r = 1$ kpc, and have assumed that the matched filter accumulates signal for an interval τ defined in equation (89) or for an interval of one year, whichever is shorter. The deformation is due to Coulomb forces, with rigidity parameters $b = 10^{-3}$, 10^{-4} and 10^{-5} as indicated. The knee that appears on the $b = 10^{-3}$ curve is due to the gravitational radiation reaction time-scale falling to below one year at high rotation rate, limiting the signal accumulated by a matched filter.
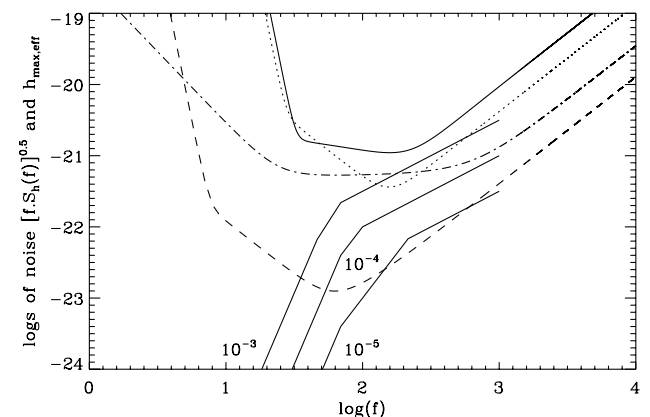
Figure 7. The effective amplitude from an isolated star with the same parameters and assumptions as in Fig. 6, except that now $n = 10^4$. This corresponds to the upper limit on n as estimated by Alpar & Sauls (1988).

7.2 Statistical arguments

Such plots as these are useful, as they show how the strength of the internal damping affects the strength of the gravitational wave signal from an isolated star. However, in order to decide whether such sources are of interest, it is necessary to consider the related issues of their event rate and distance from the Earth. To do this, we need to consider the statistics of neutron star births.

The analogous problem of the gravitational signals due to a population of young non-precessing *triaxial* neutron stars spinning down due to gravitational wave emission has been considered by Blandford, as reported in Thorne (1987). Blandford made use of the following argument. Consider a source born in a supernova explosion that is spinning down on a time-scale τ. Then there will be $\tau/\Delta t_{SN}$ such sources with age τ or younger in the Galaxy, where Δt_{SN} is the interval between Galactic supernovae. Blandford then modelled the Galaxy as a flat disc of radius R, which allowed him to estimate the distance to the *nearest* such source. He then combined this result with gravitational spin-down and wave amplitude formulae from the quadrupole formalism to show that the gravitational signal arriving at Earth from the nearest such source is proportional to $\sqrt{\Delta t_{SN}}$ and is independent of the source's frequency or triaxial ellipticity.

We wish to make the analogous argument for a population of young isolated precessing neutron stars. We will follow Blandford and consider stars where electromagnetic torques are not important. We have already shown in Section 6.2 that electromagnetic torques can, if the Goldreich pumping mechanism is active, cause young neutron stars to be set into free precession, but only at the cost of introducing a powerful spin-down torque, and so a population of unmagnetized stars is probably more easily detectable than a population of magnetized ones.

The relevant time-scale τ on which the gravitational wave signal decreases is no longer the gravitational *spin-down* time-scale, but is instead the free precession *alignment* time-scale, dominated in almost all physically plausible scenarios by internal dissipation. This means that Blandford's triaxial result where h is a function of Δt_{SN} only no longer holds.

We will model the Galaxy as having a radius R and thickness D, giving a volume of order R^2D. This contains $\tau/\Delta t_{SN}$ stars of age τ or younger. The average separation of this population of young stars is then $(\Delta t_{SN} R^2 D/\tau)^{1/3}$. Explicitly,

$$\Delta r = 1.4\,\text{kpc}\left(\frac{\Delta t_{SN}}{30\,\text{yr}}\right)^{1/3}\left(\frac{10^3\,\text{yr}}{\tau}\right)^{1/3}, \qquad (91)$$

where we have put $R = 10\,\text{kpc}$ and $D = 1\,\text{kpc}$. Of course, a more accurate model would take into account the rate of star formation as a function of Galactic position, with different rates applying in the central bulge and spiral arms, for instance. Nevertheless, equation (91) represents a useful first approximation.

Equations (36) and (37) give the wave amplitude of a precessing star in terms of r, f and τ_d. We can then set r equal to Δr as given in equation (91). The wave amplitude thus obtained will, subject to statistical variation, be the field at Earth due to the closest source of age τ_d or less. In full:

$$h = 2.4 \times 10^{-30}\,\frac{n}{10^4}\left(\frac{f}{100\,\text{Hz}}\right)^4\left(\frac{30\,\text{yr}}{\Delta t_{SN}}\right)^{1/3}\left(\frac{10^3\,\text{yr}}{\tau}\right)^{2/3} \qquad (92)$$

for $f < f_\theta$, and

$$h = 1.1 \times 10^{-30}\left(\frac{u_{break}}{10^{-3}}\right)\left(\frac{100\,\text{Hz}}{f}\right)\left(\frac{30\,\text{yr}}{\Delta t_{SN}}\right)^{1/3}\left(\frac{10^3\,\text{yr}}{\tau}\right)^{2/3} \qquad (93)$$

for $f > f_\theta$. We are considering stars with τ in excess of 30 yr, so these wave amplitudes can be compared against the noise curves for 1-yr matched filter integrations, e.g., the noise curves of Fig. 4. As can be seen, signals of $h = 10^{-27}$ lie above the Advanced LIGO noise curve for a wide range of frequencies (25 to 400 Hz), which may well include the initial spin frequencies of neutron stars. However, we are considering a 'blind search', i.e., an all-sky search without any prior knowledge of the source's position and little idea of its spin frequency. In order to minimize numerically generated false alarms, we will therefore take our detection criterion to be $h > 10^{-26}$. Also, we will set $u_{break} = 10^{-3}$. For definiteness, consider the case where all stars are born with a spin frequency $f = 100\,\text{Hz}$. If we consider the optimistic case where internal dissipation is neglected ($n \to \infty$), then the above equations show that the nearest such star is detectable for $\tau < 30\,\text{yr}$. This is on the edge of the applicability of our simple statistical model – there would only be one such star in the Galaxy! The probability of detecting such an object during the lifetime of an Advanced LIGO detector would be borderline. It follows at once that damping parameters of less than $n = 10^7$ would be unlikely to lead to a detectable population of isolated stars.

If, when the advanced detectors go on line, advances in computer power, detector noise curves or search algorithm design permit a more sensitive search down to $h = 10^{-27}$, then we obtain $\tau_d = 10^3\,\text{yr}$ for detection. There would be a population of around 30 stars of this age or less in the Galaxy. Equation (91) shows that the closest would be about 1 kpc from the Earth. Fig. 6 shows that in the case of Coulomb deformations such a star would have to have a rigidity parameter of 10^{-4}, an order of magnitude larger than the canonical value.

We are now in a position to summarize our results. We have considered the wave field due to a population of isolated stars set into precession with $\theta = \theta_{max}$ soon after birth. The signal following matched filtering is shown in Figs 6 and 7 for the case of Coulomb deformations with $u_{break} = 10^{-3}$ and $r = 1\,\text{kpc}$. They suggest that even for damping as strong as $n = 10^4$, a star with rigidity parameter $b = 10^{-4}$ is detectable out to about 1 kpc by an Advanced LIGO. However, when the statistics of neutron star births are included, it is found that with this level of internal damping it is unlikely that, at a given time, there exists such a precessing star in the Galaxy. However, the situation is very different if the internal damping is much weaker. In the limit where it negligible, with a detection threshold of 10^{-26} it is borderline as to whether or not there will exist a detectable star in the Galaxy. If this threshold can be decreased to 10^{-27}, then there could exist a detectable star as close at 1 kpc to the Earth. If deformed by Coulomb forces, such a star would require a rigidity parameter of 10^{-4} at least.

8 COLLISIONS IN DENSE ENVIRONMENTS

The possibility of detecting gravitational waves from neutron stars set into free precession following collisions with other stars has recently been discussed in the literature. De Araujo et al. (1994) first pointed out that the high stellar densities of globular clusters could lead to a high rate of collision between neutron stars and other stars. Given that globular clusters contain an excess of millisecond pulsars, the latter authors argued that if such collisions were effective in exciting precession, interesting levels of gravitational wave emission would occur.

This idea was taken up by Velloso et al. (1997), who estimated possible gravitational wave amplitudes at Earth based on the

millisecond pulsar data for the globular clusters. However, the formulae employed were taken from de Araujo et al. (1994), who effectively assumed that the stars were rigid, with an oblateness ϵ_Ω. This gave $h \propto \dot{\phi}^2 \epsilon_\Omega \theta$ and $\tau_{g,\theta} \propto 1/\epsilon_\Omega^2$. At a given wobble angle and spin frequency this led to a wave amplitude too large by a factor of $\epsilon_\Omega/\epsilon_d \approx 1/b$, and an alignment time-scale too fast by the factor $(\epsilon_\Omega/\epsilon_d)^2 \approx 1/b^2$.

In this section we will reconsider the issue of collision-induced precession. In the terminology of Section 4 this is an example of an impulsive pumping mechanism. This problem is very similar to that considered in the last section, natal precession, as we are again considering the wave field due to stars set into precession at positions and times which can only be described in a statistical way, and then spin-down and align. Indeed, the problem again breaks down neatly into two parts. The first concerns identifying particular mechanisms, i.e., types of collision, that lead to an interesting level of free precession. The second concerns finding an event rate for such an occurrence, so that a statistical statement can be made regarding the likely detectability. Note that as the nearest cluster is of order 1 kpc from the Earth, equations (36) and (37) show that a safe condition for detectability is $\tau_{g,\theta} \lesssim 10^3$ years, with the very optimistic assumptions $n = 10^7$ and a detection threshold of $h = 10^{-27}$. Additionally, we see from Fig. 6 and equation (24) that for a star with $b = 10^{-3}$ and $u_{\text{break}} = 10^{-3}$ spinning at several 100 Hz, a wobble angle of order 10^{-3} is required for a signal-to-noise ratio of 10. We therefore need to identify types of collision involving at least one recycled neutron star which produce precession angles of order 10^{-3} and have an event rate of order $1/1000 \, \text{yr}^{-1}$. These arguments are somewhat simpler than those used in the last section, but will suffice for this section, as we will find very small event rates for collision, so that it will be clear that we can rule out collisions as a mechanism for generating detectable gravitational waves.

8.1 Collisions of neutron stars with non-compact stars

We begin by considering the collision of a neutron star with a non-compact star. Such collisions have been modelled extensively, e.g. by Davies, Benz & Hills (1992), who model neutron star-main-sequence star collisions, and also neutron star–red giant collisions. In the main-sequence star case they find that a system consisting of a neutron star surrounded by a thick accretion disc is formed when the separation at periastron is $\lesssim 1.75$ times the main-sequence star's radius. In the red giant case they find that a common-envelope system is formed when the separation at periastron is $\lesssim 2.5$ times the red giant radius. For periastron separations significantly greater than these values they find that the perturbation of the non-compact star is minimal.

Despite the violent effect such near-body encounters have on the non-compact star, it is difficult to see how the neutron star would be set into free precession by such a collision. As will be shown in Section 8.2, the gravitational tidal torque on the neutron star due to the non-compact star is negligible. This leaves only the material torque on the neutron star, which will be determined by accretion flow on to its surface. This will be described by the standard theory, regardless of the unusual source of the accreting material. The accretion rate will be limited to the Eddington value in the usual manner, so the torque will not be impulsive.

It follows that although collisions between neutron stars and non-compact stars are important in terms of the population evolution of globular clusters, they are not of use as a mechanism for free precession gravitational wave production, as it is impossible to identify a way in which the collision would set the star into free precession.

8.2 Neutron star–neutron star encounters

We will now consider encounters between two neutron stars. Clearly, if a direct collision were to occur, free precession would be the last gravitational wave mechanism that we would wish to consider. We will therefore model a *near* collision, where both gravitational and magnetic effects will come into play, but there is no direct mechanical contact between the stars. We will begin by considering the gravitational interaction in a simple Newtonian way. Suppose that one star has a spin-angular momentum $\boldsymbol{J}$ and centrifugal deformation ΔI_Ω. Then the other star will exert a torque on this bulge, causing a forced precession. [It is this process that is responsible for the Earth's (forced) 'precession of the equinoxes' on a 26 000-yr time-scale, as the Sun and Moon exert a torque on the Earth's centrifugal deformation.] The magnitude of the torque acting on the star is given by (Goldstein 1980):

$$T = \frac{3GM}{2r^3} \Delta I_\Omega \sin 2\beta, \tag{94}$$

where β is the angle that the angular momentum of this star makes with the normal to the plane in which the stars move, M is the mass of the other star, and r denotes the separation of the stars. This torque acts perpendicular to the plane containing the stars and $\boldsymbol{J}$. We can write the quantity ΔI_Ω in terms of the rotation frequency Ω using equation (13):

$$\Delta I_\Omega = I \frac{3}{2} \frac{\Omega^2 R^3}{GM}. \tag{95}$$

This gives

$$T = \frac{9}{4r^3} I\Omega^2 R^3 \sin 2\beta. \tag{96}$$

As the two stars approach one another, this torque will grow and change in orientation. If the stars pass very close to one another, the steep r^{-3} factor will give rise to an almost impulsive torque, acting when the stars are at and close to periastron, where the r^{-3} factor is at a maximum. If the interval in which the bulk of the angular momentum transfer takes place is much less than the spin period of the star, the transfer will take place at nearly constant rotational phase, i.e., nearly constant reference plane orientation. It follows that the star would then be set into free precession with a wobble angle of order

$$\delta\theta \approx \frac{\delta J}{J} \frac{I}{I_{\text{crust}}} \approx \frac{T}{I_{\text{crust}}\Omega^2}. \tag{97}$$

Inserting T as given by equation (96) then gives

$$\delta\theta \approx \frac{9}{4} \left(\frac{R}{d}\right)^3 \sin 2\beta \frac{I}{I_{\text{crust}}}, \tag{98}$$

where d denotes the separation at periastron.

We therefore see that collisions capable of producing significant wobble angles ($\theta \sim 10^{-3}$) could conceivably occur, but would require very close encounters, with a periastron passage of no more than 10 neutron star radii: $d \sim 10R$. Of course, during such close passages relativistic effects will be important, e.g., Lense–Thirring precession. We need not pursue these here. All that we require is an order-of-magnitude estimate of the collision cross-section for a significant interaction to occur. Note that equation (98)

immediately rules out tidal torques during near collisions between neutron stars and main-sequence stars as a pumping mechanism, due to the large ($d \gtrsim 10^6$ km) periastron separation.

There will be an interaction between the magnetic moments of the neutron stars also, as each dipole will tend to align with the field of the other. The torque on a dipole of moment m in a field B due to the other star is of order mB. The field B scales as r^{-3}. An argument analogous to the above gravitational one then leads to a wobble angle

$$\delta\theta \approx 10^{-22} \left(\frac{B_1}{10^9 \, \text{G}}\right) \left(\frac{B_2}{10^{12} \, \text{G}}\right) \left(\frac{100 \, \text{Hz}}{f}\right)^2 \left(\frac{10 \, \text{km}}{d}\right)^3, \qquad (99)$$

where B_1 and B_2 denote the *polar* field strengths of the two stars. We have parameterized in terms of field strengths appropriate for a collision between a recycled and non-recycled neutron star. This is much smaller than the gravitationally induced wobble angle, and need not be considered further.

Having established that near collisions could excite free precession, we must now consider an event rate for such close passages. Of course, given that the event rate for encounters between a neutron star and a non-compact star was low, it is clear that the event rate for such close neutron star–neutron star encounters will be extremely low. In fact, it is straightforward to show that no such near-collisions will occur over a Hubble time, using a simple model. Suppose that there are N neutron stars in a globular cluster of size R_{gc}. Let v_∞ denote their average velocity when far apart. Then in a unit time this population sweeps out an effective volume of order NAv_∞, where A is a collision cross-section. Then the probability of a *given* neutron star colliding with another in this interval is of the order of this volume divided by the globular cluster volume, i.e., of order $NAv_\infty/R_{\text{gc}}^3$. As there are N such stars, the probability of *any one of them* colliding with any other is then N times this, giving a collision rate $N^2Av_\infty/R_{\text{gc}}^3$. As there are approximately 200 globular clusters in the Galaxy, we obtain a Galactic collision rate $\nu_{\text{collision}}$:

$$\nu_{\text{collision}} \approx 200 \frac{N^2 A v_\infty}{R_{\text{gc}}^3}. \qquad (100)$$

If gravitational attractions were neglected, the collision cross-section would be of order $d^2 \sim (100 \, \text{km})^2$. However, gravitational focusing will increase the effective cross-section, as described in Verbunt & Hut (1987):

$$A \approx d^2 \left(1 + \frac{2GM_{\text{total}}}{v_\infty^2 d}\right), \qquad (101)$$

where M_{total} denotes the sum of the masses of the two stars. The second term on the right-hand side describes the effects of gravitational focusing. For the case of interest it is the dominant factor. Parametrizing, we find an event rate

$$\nu_{\text{collision}} \sim 10^{-11} \, \text{yr}^{-1} \left(\frac{N}{10^3}\right)^2 \left(\frac{M_{\text{total}}}{2.8 \, M_\odot}\right) \left(\frac{d}{100 \, \text{km}}\right)$$

$$\times \left(\frac{10 \, \text{km}}{v_\infty}\right) \left(\frac{1 \, \text{pc}}{R_{\text{gc}}}\right)^3. \qquad (102)$$

Such an event rate as this makes further comment unnecessary, save to say that we will not consider stellar collisions any further.

9 CONCLUSIONS

This paper represents a systematic analysis of the detectability of gravitational waves from freely precessing neutron stars. It is based upon a model commonly employed to describe the Earth's own motion. Explicitly, the neutron star has been modelled as an elastic shell with a fluid core, whose angular amplitude of free precession (the *wobble angle*) is limited by its finite crustal lattice strength. It has been known for some time that neutron star structure may well allow detectable gravitational wave signals at Earth, but this is the first study to attempt to identify particular astrophysical scenarios in which such precessional motion might be brought about and/or maintained.

Broadly speaking, our findings were pessimistic. It proved impossible to find astrophysical pumping mechanisms capable of giving steady gravitational wave amplitudes detectable by an *Advanced* LIGO. This was because of the limiting effect of dissipation mechanisms internal to the star, even when dissipation strengths several orders of magnitude smaller than theoretically estimated values were assumed.

Two qualifications are in order. First, the above conclusions were reached for stars with oblate deformations. In the physically less likely case of a star with a prolate deformation, the effect of internal dissipation would be to *increase* the wobble angle. Such a situation is certainly interesting from the gravitational wave point of view, although the dynamics of such a star, possibly involving crust cracking when the wobble angle exceeds a critical value, are far from clear. Secondly, most of the pumping mechanisms considered in this paper involved an externally generated torque being exerted on the star. There exists another possibility, where the symmetry axis of the deformation shifts due to a smooth plastic deformation of the crust. For instance, this deformation might be caused by accretion-induced temperature or composition asymmetries, in the manner described by Bildsten (1998) for non-precessing triaxial stars. These two possible modifications to our model are currently under investigation, to see if there may yet prove to be a way of powering a long-lived, freely precessing gravitational wave source.

REFERENCES

Alpar A., Pines D., 1985, Nat, 314, 334
Alpar A., Sauls J. A., 1988, ApJ, 327, 723
Andersson N., Kokkotas K. D., 2001, Int. J. Mod. Phys., 10, 381
Andersson N., Jones D. I., Kokkotas K. D., Stergioulas N., 2000, ApJ, 534, L75
Baym B., Pines D., 1971, Annals of Physics, 66, 816
Bildsten L., 1998, ApJ, 501, L89
Bondi H., Gold T., 1955, MNRAS, 115, 41
Cutler C., Jones D. I., 2000, Phys. Rev. D, 63, 024002
Davies M. B., Benz W., Hills J. G., 1992, ApJ, 401, 246
Davis L., Goldstein M., 1970, ApJ, 159, L81
de Araujo J. C. N., de Freitas Pacheco J. A., Horvath J. E., Cattini M., 1994, MNRAS, 271, L31
Deutsch A. J., 1955, Annales d'Astrophysique, 18, 1
Flanagan È. È., 1998, in Dadhich N., Narlikar J., eds, Gravitation and Relativity: At the turn of the Millennium, Proceedings of the 15th

International Conference on General Relativity and Gravitation (GR15). IUCAA, p. 177

Goldreich P., 1970, ApJ, 160, L11

Goldreich P., Julian W. H., 1969, ApJ, 157, 869

Goldstein H., 1980, Classical Mechanics. Addison-Wesley

Good M. L., Ng K. K., 1985, ApJ, 299, 706

Haensel P., 1997, in Marck J.-A., Lasota J.-P., eds, Relativistic Gravitation and Gravitational Radiation, Les Houches, 1995, p. 129

Jones D. I., 2000, PhD thesis, Univ. Wales, Cardiff

Jones D. I., Andersson N., 2001, MNRAS, 324, 811

Lamb D. Q., Lamb F. K., Pines D., Shaham J., 1975, ApJ, 198, L21

Lamb F. K., Shibazaki N., Alpar M. A., Shaham J., 1985, Nat, 317, 681

Landau L. D., Lifshitz E. M., 1976, Mechanics, 3rd Edition. Butterworth-Heinemann Ltd, London

Lindblom L., Owen B. J., Ushomirsky G., 2000, Phys. Rev. D, 62, 084030

Link B., Franco M. L., Epstein R. I., 1998, ApJ, 508, 838

Lyne A. G., 1996, in Johnston S., Walker M. A., Bailes M., eds, ASP Conf. Ser. Vol. 105, Pulsars: Problems and Progress. Astron. Soc. Pac., San Francisco, p. 73

Melatos A., 1999, ApJ, 519, L77

Michel F. C., 1991, Theory of Neutron Magnetospheres. Univ. Chicago Press, Chicago

Michel F. C., Goldwire H. C., 1970, Astrophys. Lett., 5, 21

Misner C. W., Thorne K. S., Wheeler J. A., 1973, Gravitation. Freeman, San Francisco

Ostriker J., Gunn J., 1969, ApJ, 157, 1395

Owen B. J., Sathyaprakash B. S., 1999, Phys. Rev. D, 60, 022002

Papaloizou J., Pringle J. E., 1978, MNRAS, 184, 501

Pines D., Shaham J., 1972a, Nat. Phys. Sci., 235, 43

Pines D., Shaham J., 1972b, Phys. Earth Planet. Interiors, 6, 103

Pines D., Shaham J., 1973a, Nat. Phys. Sci., 243, 122

Pines D., Shaham J., 1973b, Nat, 245, 77

Ruderman M., 1976, ApJ, 203, 213

Ruderman M., 1991a, ApJ, 366, 261

Ruderman M., 1991b, ApJ, 382, 576

Ruderman M., 1992, in Pines D., Tamagaki R., Tsuruta S., eds, Structure and Evolution of Neutron Stars. Addison-Wesley, Redwood CA, p. 353

Schutz B. F., 1991, in Blair D., ed., The Detection of Gravitational Radiation. Cambridge Univ. Press, Cambridge, p. 406

Shaham J., 1977, ApJ, 214, 251

Shapiro S. L., Teukolsky S. A., 1983, Black Holes, White Dwarfs, and Neutron Stars. Wiley-Interscience, New York

Thorne K. S., 1987, in Hawking S. W., Israel W., eds, 300 Years of Gravitation. Cambridge Univ. Press, Cambridge, p. 330

Ushomirsky G., Cutler C., Bildsten L., 2000, MNRAS, 319, 902

Velloso W., Barone F., Calloni E., Fiore L. D., Garufi F., Grado A., Milano L., 1997, in Bassan M., Ferrari V., Francaviglia M., Fucito F., Modena I., eds, General Relativity and Gravitational Physics: Proceedings of the 12th Italian Conference. World Scientific Press, London, p. 457

Verbunt F., Hut P., 1987, in Helfand J., Huang J.-H., eds, Proc. IAU Symp. 125, The Origin and Evolution of Neutron Stars. Reidel, Dordrecht, p. 187

Vietri M., Stella L., 1998, ApJ, 503, 350

Wagoner R. V., 1984, ApJ, 278, 345

Wang Y.-M., Robnik M., 1982, Astron. Astrophys., 107, 222

Zimmermann M., 1978, Nat, 271, 524

Zimmermann M., Szedenits E., Jr., 1979, Phys. Rev. D, 20, 351

This paper has been typeset from a TEX/LATEX file prepared by the author.